Combined Mesenchymal Stromal Cell Therapy and ECMO in ARDS

Combined Mesenchymal Stromal Cell Therapy and ECMO in ARDS: A Controlled Experimental Study in Sheep

Jonathan E Millar[1,2,3], Nicole Bartnikowski[1,4], Margaret R Passmore[1,2], Nchafatso G Obonyo[1,5], Maximillian V Malfertheiner[1,6], Viktor von Bahr[1,7], Meredith A Redd[8], Louise See Hoe[1,2], Katrina K Ki[1,2], Sanne Pedersen[1,4], Andrew J Boyle[3], J Kenneth Baillie[9], Kiran Shekar[1,2], Nathan Palpant[8], Jacky Y Suen[1,2], Michael A Matthay[10], Daniel F McAuley[3], John F Fraser[1,2] on behalf of the Combining Extracorporeal Life Support and Cell Therapy in Critical Illness (CELTIC) investigators.

[1] Critical Care Research Group, The Prince Charles Hospital, Brisbane, Australia.

[2] Faculty of Medicine, University of Queensland, Australia.

[3] Wellcome-Wolfson Institute for Experimental Medicine, Queen's University Belfast, United Kingdom.

[4] Institute of Health and Biomedical Innovation, Queensland University of Technology, Australia.

[5] Wellcome Trust Centre for Global Health Research, Imperial College London, United Kingdom.

[6] Department of Internal Medicine II, Cardiology and Pneumology, University Medical Center Regensburg, Germany.

[7] Department of Physiology and Pharmacology, Section for Anesthesiology and Intensive Care Medicine, Karolinska Institutet, Stockholm, Sweden.

[8] Institute for Molecular Bioscience, University of Queensland, Australia.

[9] Roslin Institute, University of Edinburgh, United Kingdom

AJRCCM Articles in Press. Published April 15, 2020 as 10.1164/rccm.201911-2143OC

[10] Departments of Medicine and Anesthesia, Cardiovascular Research Institute, University of California, San Francisco, United States of America.

Corresponding author

Dr Jonathan E. Millar

Critical Care Research Group

The Prince Charles Hospital,

Chermside, Brisbane, Queensland, Australia, 4032

Telephone: +44 (0) 7545579065

Email: j.millar@doctors.org.uk

Authors contributions

J.E.M. – study conception, model development, study design and conduct, animal surgery, data collection and analyses, manuscript preparation.

N.B., J.Y.S. – model development, study design and conduct, data collection and analyses, manuscript review.

N.G.O., M.V.M., V.vB. – model development, study design and conduct, animal surgery, manuscript review.

M.A.R., M.R.P., K.K.K. – sample analyses, data analyses, manuscript review.

S.P. - model development, study design and conduct, animal surgery, manuscript review.

J.K.B. – data analysis, manuscript review.

N.P., A.J.B, M.A.M. - study design, data interpretation, manuscript review.

D.F.M., J.F.F. - study conception, model development, study design, data interpretation, manuscript review.

AJRCCM Articles in Press. Published April 15, 2020 as 10.1164/rccm.201911-2143OC

Funding sources

We gratefully acknowledge funding from the Intensive Care Society (UK), The Prince Charles Hospital Foundation, the Queensland Government, and the National Health and Medical Research Council (Australia). We also acknowledge the endorsement of this study by the International ECMO Network (ECMONet). Mesenchymal stromal cells were donated in-kind, under a material transfer agreement, by Cynata Therapeutics Ltd., Melbourne, Australia. Cynata Therapeutics Ltd. was not involved in the conception, design, or analysis of the study. Prof. Matthay is supported by NHLBI HL123004, HL140026, HL126456.

Running title

Combined MSC therapy and ECMO in experimental ARDS

Subject category classification

4.1 ALI/ARDS: Biological Mechanisms

Manuscript word count

3,086 words

At a glance commentary

Scientific knowledge on the subject:

Mesenchymal stromal cell (MSC) therapy is a promising novel intervention for ARDS. Trials to date have failed to explore the safety of cell therapy during ECMO. Pre-clinical investigations have found that MSC therapy during ECMO attenuate the efficacy of ECMO.

What this study adds to the field:

This study, employing a 24-hour, large animal model of ARDS and ECMO, examined the safety and efficacy of MSC therapy. We found that endobronchially administered MSCs adhere

AJRCCM Articles in Press. Published April 15, 2020 as 10.1164/rccm.201911-2143OC

to, and impair, membrane oxygenators *in-vivo*. MSCs did not improve oxygenation or other ventilatory parameters but did reduce the severity of histological evidence of lung injury. Our data also suggest that MSCs may reduce circulatory shock associated with ARDS. There were no adverse effects of MSC administration on renal or liver function.

Online data supplement

This article has an online data supplement, which is accessible from this issue's table of content online at www.atsjournals.org.

AJRCCM Articles in Press. Published April 15, 2020 as 10.1164/rccm.201911-2143OC

Abstract

Rationale

Mesenchymal stromal cell therapy is a promising intervention for ARDS, although trials to date have not investigated its use alongside ECMO. Recent pre-clinical studies have suggested that combining these interventions may attenuate the efficacy of ECMO.

Objectives

To determine the safety and efficacy of mesenchymal stromal cell therapy in a model of ARDS and ECMO.

Methods

ARDS was induced in 14 sheep, after which they were established on veno-venous ECMO. Subsequently, they received either, endobronchial iPSC-derived human MSCs (hMSCs, n=7) or cell-free carrier vehicle (Vehicle control, n=7). During ECMO, a low tidal volume ventilation strategy was employed in addition to protocolized hemodynamic support. Animals were monitored and supported for 24 hours. Lung tissue, bronchoalveolar fluid, and plasma were analysed, in addition to continuous respiratory and hemodynamic monitoring.

Measurements and main results

The administration of hMSCs did not improve oxygenation (PaO_2/FiO_2 mean difference -146 mmHg, $p = 0.076$) or pulmonary function. However, histological evidence of lung injury (Lung Injury Score mean difference -0.07, $p = 0.04$) and BAL IL-8 were reduced. In addition, hMSC treated animals had a significantly lower cumulative requirement for vasopressor. Despite endobronchial administration, animals treated with hMSCs had a significant elevation in trans-membrane oxygenator pressure gradients. This was accompanied

AJRCCM Articles in Press. Published April 15, 2020 as 10.1164/rccm.201911-2143OC

by more pulmonary artery thromboses and adherent hMSCs found on explanted oxygenator fibers.

Conclusions

Endobronchial hMSC therapy in an ovine model of ARDS and ECMO can impair membrane oxygenator function and does not improve oxygenation. These data do not recommend the safe use of hMSCs during VV-ECMO.

Abstract word count

250

Keywords

Acute Respiratory Distress Syndrome

Extracorporeal membrane oxygenation

Mesenchymal stromal cells

Models, Animal

AJRCCM Articles in Press. Published April 15, 2020 as 10.1164/rccm.201911-2143OC

Introduction

The quest for an effective pharmacological treatment for the Acute Respiratory Distress Syndrome (ARDS) has been unsuccessful. Recently, mesenchymal stromal cells (MSCs) have attracted attention as a candidate therapy for ARDS (1).

MSCs are multipotent adult stem cells found in tissues of mesodermal origin such as bone marrow (2). Therapeutic interest in these cells has arisen because of their pleiotropic immunomodulatory abilities. During acute inflammation, MSCs appear to be immunosuppressive, influencing both innate and adaptive immune responses (3). In ARDS, their beneficial effects are believed to be mediated in a variety of ways, including; secretion of anti-inflammatory paracrine factors (4), restoration of epithelial and endothelial integrity (5), enhancement of alveolar fluid clearance (6), direct antimicrobial activity (7), and by mitochondrial transfer (8). In pre-clinical models of acute lung injury, MSCs have been shown to reduce mortality (9). A phase 2 study has been conducted in patients with ARDS with no reported infusion-related adverse events (10).

To date, trials of MSCs in ARDS have excluded patients supported with extracorporeal membrane oxygenation (ECMO). The use of ECMO in acute severe respiratory failure has increased substantially in the last decade and is now an established tool for supporting those with refractory illness (11). The use of MSCs during ECMO, while potentially attractive, raises some unique considerations. Firstly, MSCs are large cells, with an average diameter between 10-30 μm (12), which when administered therapeutically may pose a risk to the patency of a membrane oxygenator. Secondly, a defining characteristic of MSCs is avid plastic adherence (13); this too may threaten membrane oxygenators, which are constructed largely from plastics. Recent *ex-vivo* and small animal experimentation has confirmed these concerns (14, 15).

AJRCCM Articles in Press. Published April 15, 2020 as 10.1164/rccm.201911-2143OC

Conversely, immunomodulation by MSCs may provide additional benefits for ECMO patients, where the institution of extracorporeal support results in an additional inflammatory insult (16).

Given the paucity of evidence to support the safe use of MSC therapy during ECMO, we conducted a controlled trial of clinical-grade induced pluripotent stem cell (iPSC) derived human MSCs (hMSCs) in an ovine model of ARDS, supported with veno-venous ECMO (VV-ECMO). The primary objective was to assess the safety of MSC therapy and to investigate its effect on physiologic and biologic markers of pulmonary and systemic injury.

Methods

Study design

Ethical approvals were obtained from University Animal Ethics Committees (QUT1600001108, UQPCH/483/17) and authorization for *in-vivo* use of hMSCs was granted by the Australian Department of Agriculture (2017/075). The study was conducted in accordance with the Australian Code of Practice for the Care and Use of Animals for Scientific Purposes (17) and is reported in compliance with ARRIVE guidelines (18). Detailed methods and a comprehensive description of the experiments and analyses are provided in an online supplement. A schematic of the study protocol is provided in **Figure 1**.

Animal model

Fourteen healthy Border Leicester Cross ewes aged between 1-3 years and weighing between 46-55 kg (mean, 52.6 ± 3 kg), were randomly assigned to one of two groups; endobronchial iPSC-derived hMSC treatment (n=7) or endobronchial carrier vehicle only (n=7).

In brief, animals were anesthetized with a combination of ketamine, midazolam, and fentanyl. Continuous neuromuscular blockade was maintained by infusion of vecuronium. In a

AJRCCM Articles in Press. Published April 15, 2020 as 10.1164/rccm.201911-2143OC

supine position, animals were tracheostomized and ventilated using a low tidal volume strategy (6 mL/kg actual body weight (ABW)). After instrumentation, acute lung injury was induced by combining an intravenous infusion of oleic acid (OA; 0.06 mL/kg; O1008, Sigma-Aldrich, Castle Hill, NSW, Australia) with endobronchial *E. coli* lipopolysaccharide (LPS; 100 µg; O55:B5, Sigma-Aldrich, Castle Hill, NSW, Australia). Once a PaO_2/FiO_2 ratio < 100 mmHg (PEEP ≥ 10 cmH_2O) was obtained (T_0), animals were established on VV-ECMO via a right-sided jugular-jugular configuration (T_1) and positioned in sternal recumbency. VV-ECMO was combined with a lower tidal volume strategy (4 mL/kg ABW) for 22 hours, at which time (T_{23}) ECMO was stopped and a standardized recruitment manoeuvre was performed. Animals were returned to pre-ECMO ventilatory settings for one hour before being euthanized (T_{24}).

iPSC-derived hMSCs

After one hour of VV-ECMO (T_2), animals received a fixed dose of 3 x 10^8 iPSC-derived hMSCs suspended in a carrier vehicle (hMSC) or carrier vehicle alone (Vehicle control). Cells were provided by Cynata Therapeutics Ltd. (CYP-001; Cynata Therapeutics Ltd., Melbourne, VIC, Australia). These cells were ≥ 99% positive for CD-73, CD-90, and CD-105, but negative for CD-31 and CD-45. The total volume of vehicle was 60 mL (57.5% Plasmalyte-A, 40% Flexbumin 25%, 2.5% Dimethyl sulfoxide). Cells were ≥ 97% viable prior to administration. The distribution of delivery is described in **Figure E1**.

Statistical analysis

An *a priori* sample size calculation, based on the primary outcome of PaO_2/FiO_2 ratio at 24 hours, is detailed in the online supplement. Data are expressed as mean (± SD) or median (IQR) if non-normally distributed. Analysis was undertaken in Graphpad Prism (v 8.1.2., GraphPad Software, San Diego, USA). Longitudinal data were analyzed by fitting a mixed model. This model uses a compound symmetry covariance matrix and is fit using restricted

AJRCCM Articles in Press. Published April 15, 2020 as 10.1164/rccm.201911-2143OC

maximum likelihood. Where a significant interaction was observed *post-hoc* comparisons were undertaken. Correction for multiple comparisons was made using the Benjamini-Hochberg method (false discovery rate restricted to 5%). Non-longitudinal data were compared using an unpaired t-test or a Mann-Whitney test as appropriate. Categorical data were compared using the chi-squared test. Statistical significance was assumed if $P < 0.05$.

Results

Baseline characteristics at injury (T_0) are shown in **Table 1** and in **supplementary Table E1**. All animals completed the study protocol and were euthanized at T_{24}.

Respiratory variables

The use of ECMO facilitated a lower tidal volume ventilation strategy (4 (4-4) mL/kg ABW). The median ECMO flow rate was 2.75 L/min (2.5-3.25 L/min), with a sweep gas flow of 3 L/min (2-3.5 L/min). During VV-ECMO, animals had a median PaO_2 of 109 mmHg (94-131 mmHg) and a $PaCO_2$ of 32 mmHg (30-35 mmHg). There were no significant differences in these parameters between groups (**supplementary Figure E2**). Animals were adequately anticoagulated during ECMO, as measured by activated partial thromboplastin time (aPTT) ratios. The dose of heparin was not significantly different between groups (**supplementary Figure E2**).

Because VV-ECMO controls gas exchange, native lung function was assessed one hour after cessation of extracorporeal flow and after the performance of a standardized lung recruitment manoeuvre (T_{24}). As shown in **Figure 2** both the PaO_2/FiO_2 ratio ($p = 0.076$) and the oxygenation index (OI) ($p = 0.153$) were numerically better in the carrier vehicle only group, the differences were not statistically significant.

AJRCCM Articles in Press. Published April 15, 2020 as 10.1164/rccm.201911-2143OC

The plateau airway and driving pressures were similar between groups at T_{24} (**Figure 2**). Static lung compliance was also similar, both during and after ECMO (**Figure 2)**. The use of a protocolized recruitment manoeuvre did not improve compliance after cessation of extracorporeal support in either group (**Figure 2**).

Hemodynamic variables

This model of acute lung injury was associated with the development of hyperdynamic shock, which worsened over time (**Figure 3**). The administration of hMSCs resulted in significantly lower cumulative vasopressor doses (**Figure 3)**. At T_4, mean arterial pressure (MAP) was significantly higher in the hMSC treated group ($p = 0.001$), even though these animals received lower doses of noradrenaline (Figure 3). By T_{14}, MAP was again similar between groups, although vasopressor requirements continued to be lower in hMSC treated animals. In addition, there were lower arterial lactate concentrations, higher arterial base excesses, and lower mean pulmonary artery pressures from 12 hrs (T_{14}) post instillation in the hMSC group (**Figure 3**), however these were not statistically significant. Cumulative fluid balance at T_{24} was similar in both groups (Vehicle control, 2713 ± 970 mL vs. hMSCs, 2992 ± 1237 mL, $p = 0.648$).

Histopathology and lung injury

The blinded assessment of lung tissue was conducted by an independent expert veterinary pathologist. Sections of the right lower lobe were prepared, and a lung injury score (LIS) was calculated (19). The administration of hMSCs resulted in significantly lower scores ($p = 0.04$) (**Figure 4**), principally mediated by a reduction in neutrophil infiltration.

There were no significant differences in lung wet/dry ratio or bronchoalveolar lavage (BAL) total protein concentration (**Figure 4**). BAL fluid inflammatory cell counts are detailed in **supplementary Table E4**. There were no significant differences in these counts over time.

AJRCCM Articles in Press. Published April 15, 2020 as 10.1164/rccm.201911-2143OC

Similarly, there was no difference in lung tissue homogenate gene expression (as assessed by qPCR) between groups (**supplementary Figure E3**).

In a *post-hoc* analysis, pulmonary arterial thrombosis was noted in 5 hMSC treated animals, but only one animal receiving carrier vehicle alone ($p = 0.031$).

Inflammatory cytokines

BAL and plasma cytokine concentrations were assessed longitudinally **(supplementary Figure E4 and supplementary Figure E5**). In BAL, statistically significant differences in IL-8 were observed at T_3, T_{14}, and T_{23} ($p = 0.013$, 0.016, and 0.028 respectively). In plasma, cytokine trajectories were similar between groups (**supplementary Figure E5**).

Hematological and biochemical measurements

A summary of hematological and biochemical values are provided in **supplementary Tables E2** and **E3**. This lung injury model was associated with the development of acute kidney injury and abnormal liver function, although there were no significant differences in indices between groups. The administration of hMSCs resulted in a significantly lower lymphocyte count at T_{24} ($p = 0.047$) (**supplementary Figure E5**).

Cell-ECMO membrane interaction and cell fate

The administration of hMSCs was associated with a significant increase in the trans-oxygenator pressure gradient, becoming apparent 4 hours after cell delivery (**Figure 5**). By T_{23}, the mean pressure gradient in the hMSC group reached 64 ± 37 mmHg vs. 17 ± 9 mmHg in the vehicle only group. The instillation of carrier vehicle alone was associated with a reduction in the ECMO pump speed to flow ratio over time, a finding not observed in the hMSC group (**Figure 5**). During the study, there were no instances of pump or oxygenator failure requiring

AJRCCM Articles in Press. Published April 15, 2020 as 10.1164/rccm.201911-2143OC

a component exchange. Likewise, there was no evidence of clotting on the oxygenator surface by visual examination in either group.

Membrane oxygenators from animals treated with hMSCs were isolated and preserved at the termination of ECMO, subsequent deconstruction and staining of the fiber bundles (n=7) revealed adherent cells exhibiting surface markers consistent with those of hMSCs (**supplementary Figure E6**). Similar cell populations were not apparent in vehicle only controls (n=3).

Discussion

We carried out a trial of clinical-grade iPSC-derived hMSCs, given endobronchially, for acute lung injury in sheep during VV-ECMO. The main findings of this study can be summarized as follows; (1) with regard to the primary outcome, hMSCs did not improve oxygenation at 24 hours. (2) hMSCs did not improve pulmonary mechanics but did improve the severity of histological lung injury and reduced the concentration of bronchoalveolar lavage IL-8. (3) in spite of endobronchial administration, hMSCs adhered to and impacted the function of a commercial membrane oxygenator *in-vivo* - with an increase in the trans-membrane oxygenator pressure gradient. In addition, more pulmonary arterial thromboses were noted in hMSC-treated lungs. (4) hMSCs reduced the depth and severity of shock.

This study was conducted in a large animal model of ARDS and ECMO, which replicates several important clinical features (20). The 'double-hit' injury applied in this study resulted in acute severe hypoxemic respiratory failure consistent with modern criteria for the use of VV-ECMO (11). To support the severe acute respiratory failure, we employed a commercial ECMO device which is in widespread clinical use. Additionally, our protocolized intensive care was consistent with clinical best practice standards (21). A common criticism of pre-clinical trials of MSCs has been the use of heterogeneous, non-clinical grade cell products

AJRCCM Articles in Press. Published April 15, 2020 as 10.1164/rccm.201911-2143OC

(1), however, we tested a commercial hMSC product which is under investigation in clinical trials.

MSCs have been administered to patients with respiratory failure on ECMO (22, 23). These reports, which include only three patients, did not describe infusion-related adverse events although failed to fully characterize the interaction between MSCs and the extracorporeal device. Kocyildrim *et al*. have conducted the only other pre-clinical study involving both MSCs and ECMO for respiratory failure (24). Their ovine based, 6-hour pilot study did not report on the impact of MSC administration on the performance of ECMO.

hMSCs and pulmonary function

In this study, the administration of hMSCs failed to improve oxygenation at T_{24}. Furthermore, animals receiving hMSCs had a trend for worse oxygenation index values. In a phase 2a study of 60 patients with ARDS, the intravenous administration of hMSCs did not significantly improve PaO_2/FiO_2 ratio, although there was a signal toward improvement in oxygenation index in a *post-hoc* analysis (10). Pre-clinical studies of MSCs in ARDS have reported improvements in oxygenation, although few have produced lung injury as severe (25). In a recent systematic review of pre-clinical models combining ARDS and ECMO, only four achieved PaO_2/FiO_2 values <100 mmHg (20). The degree of lung injury in this model may explain why oxygenation is impaired in the treated group, despite improvements in inflammation and lung injury. Emerging research has highlighted the pro-coagulant effects of transplanted MSCs. These appear to be primarily mediated by MSC expression of tissue factor (26), but also by the secretion of pro-coagulant microvesicles (27) and by direct enhancement of platelet deposition (28). In pre-clinical experiments MSCs have been associated with the development of pulmonary emboli *in-vivo* (29). In this study, despite the use of heparin, almost all hMSC animals (n=6) had histological evidence of pulmonary arterial thrombosis at post-

AJRCCM Articles in Press. Published April 15, 2020 as 10.1164/rccm.201911-2143OC

mortem. The presence of exogenous hMSCs within the disordered pulmonary vasculature may have contributed to impairments in oxygenation, tempered by the fact that there was no increase in mean pulmonary artery pressure in treated animals.

Animals receiving hMSCs had improved composite histologic lung injury scores at post-mortem. The components of the score most influenced by hMSCs were neutrophil numbers in the alveolar and interstitial space. Multiple studies of MSCs in pre-clinical models of ARDS have demonstrated their ability to reduce neutrophil infiltration (30) and neutrophil extracellular trap formation (31). In this study, BAL neutrophil counts did not differ between groups. This may reflect the technical challenges of obtaining and assessing BAL cell counts. In a recent porcine model of ARDS and MSC therapy, a reduction in neutrophil infiltration was correlated with a reduction in BAL IL-8 concentrations (32), a finding confirmed in this study.

hMSCs and the systemic inflammatory response

Multiple pre-clinical models (33) and recent clinical trials (34-37) have examined the use of MSCs in the treatment of septic shock. Animals receiving hMSCs required less vasopressor support throughout the experiment to achieve an equivalent or higher MAP. A similar, early but non-sustained, reduction in vasopressor requirement has previously been described in a large-animal model of septic shock treated with MCSs (38). hMSCs did not alter plasma concentrations of pro-inflammatory cytokines over extended time periods in this study, a finding which has previously been identified in other pre-clinical (39) and clinical studies (34). A recent Phase I dose escalation study of MSCs in patients with septic shock demonstrated that the maximum effect of cell therapy on plasma cytokine levels occurred at 4 hours post-administration and declined with time (36). In this study, that time period coincides with the maximum separation in vasopressor dose, MAP, and levels of IL-1β and IL-6 between

AJRCCM Articles in Press. Published April 15, 2020 as 10.1164/rccm.201911-2143OC

groups. This may indicate that repeat dosing of MSCs will be required for optimal therapeutic efficacy.

hMSCs and ECMO

The risk posed by MSCs to membrane oxygenators has been postulated for some time (1), but has only recently been shown to have an experimental basis. Our group has previously reported the ability of hMSCs to tightly adhere to the membrane fibers of a commercial oxygenator. This may have been the result of the known plastic avidity of MSCs (13). Recently, Cho *et al.* reported the loss of systemically administered MSCs in an *ex-vivo* model of veno-arterial ECMO (15).

Given the emerging signal that systemically administered MSCs may interact with membrane oxygenators, we decided to test endobronchial instillation in this study. Cardenes *et al*. have used 18F-fluorodeoxyglucose labelling to track the fate of both systemically and endobronchially administered MSCs in an ovine model of ARDS (40). While systemically administered cells have a wide biodistribution in the first 5 hours, endobronchially administered cells were retained at the site of instillation. There are key differences in our approach, including the means of inducing lung injury and its severity.

Limitations

This study has some limitations. First, while our model of injury replicates several relevant features including severe respiratory and hemodynamic failure, clinical ARDS is usually caused by infection and develops over several days, often in patients with other comorbidities (41). Second, MSCs are known to exhibit different functional responses dependent on the contemporary milieu, which in some circumstances may be detrimental (42). This study may have modelled only one phase of acute lung injury and so hMSCs may have exerted an effect which may differ in other phases. Third, while our model extended 21 hours

AJRCCM Articles in Press. Published April 15, 2020 as 10.1164/rccm.201911-2143OC

post cell or vehicle delivery, this may have been too short a period to observe some beneficial effects of the intervention. For example, it may be that the favourable effect of hMSCs on histological injury may have translated to improvements in oxygenation over a longer time period. Conversely, an extension of the study period in the face of rising trans-oxygenator pressure gradients in the hMSC group may have ultimately led to circuit failures. Fourth, the use of a lung recruitment maneuver and the assessment of native lung function off ECMO may have had several adverse effects and we cannot be certain that these effects did not differ between groups. This approach was taken due to the challenge of assessing native lung function during ECMO, particularly where a lower tidal volume ventilatory strategy has been adopted. The study protocol was designed prior to the publication of the ART randomized controlled trial (43). Fifth, the addition of an uninjured control group may have provided further insights into the distribution of hMSCs during VV-ECMO. Finally, the dose and method of delivery of hMSCs remain a matter of conjecture. Based on the findings of our previous work (14), we chose not to investigate intravenous administration. Likewise, based on clinical trial experience, we opted to administer a single, fixed-dose of hMSCs. It is possible that varying the dose and/or route of administration of hMSCs may alter their efficacy and safety profile during ECMO.

Conclusion

In a 24-hour, ovine model of ARDS and VV-ECMO, we found that hMSC therapy was associated with impairment of the membrane oxygenator. The use of cell therapy did not result in improvements in oxygenation, the primary outcome of this study, but was associated with a reduction in histological evidence of lung injury and inflammation in the lung. Given these data we cannot currently recommend the administration of hMSCs during ECMO.

AJRCCM Articles in Press. Published April 15, 2020 as 10.1164/rccm.201911-2143OC

Acknowledgments

We are grateful for assistance provided during animal experiments by the staff of the Queensland University of Technology Medical Engineering Research Facility (MERF) and the University of Queensland Animal Science Precinct (QASP). We extend our thanks to Ms Arlanna Esguerra-Lallen for providing expert nursing care and to Ms Mengyao Yang, Mr Matthew Wells, Dr Ai-Ching Boon, Mr Michael Cavaye, and Ms Ashlen Garrett for their assistance in study preparation, sampling, and laboratory analyses.

AJRCCM Articles in Press. Published April 15, 2020 as 10.1164/rccm.201911-2143OC

References

1. Millar JE, Fraser JF, McAuley DF. Mesenchymal stromal cells and the acute respiratory distress syndrome (ARDS): challenges for clinical application. *Thorax* 2015; 70: 611-612.

2. Pittenger MF, Mackay AM, Beck SC, Jaiswal RK, Douglas R, Mosca JD, Moorman MA, Simonetti DW, Craig S, Marshak DR. Multilineage potential of adult human mesenchymal stem cells. *Science* 1999; 284: 143-147.

3. Curley GF, McAuley DF. Stem cells for respiratory failure. *Curr Opin Crit Care* 2015; 21: 42-49.

4. Devaney J, Horie S, Masterson C, Elliman S, Barry F, O'Brien T, Curley GF, O'Toole D, Laffey JG. Human mesenchymal stromal cells decrease the severity of acute lung injury induced by E. coli in the rat. *Thorax* 2015; 70: 625-635.

5. Fang X, Neyrinck AP, Matthay MA, Lee JW. Allogeneic human mesenchymal stem cells restore epithelial protein permeability in cultured human alveolar type II cells by secretion of angiopoietin-1. *J Biol Chem* 2010; 285: 26211-26222.

6. McAuley DF, Curley GF, Hamid UI, Laffey JG, Abbott J, McKenna DH, Fang X, Matthay MA, Lee JW. Clinical grade allogeneic human mesenchymal stem cells restore alveolar fluid clearance in human lungs rejected for transplantation. *Am J Physiol Lung Cell Mol Physiol* 2014; 306: L809-815.

7. Krasnodembskaya A, Song Y, Fang X, Gupta N, Serikov V, Lee J-W, Matthay MA. Antibacterial effect of human mesenchymal stem cells is mediated in part from secretion of the antimicrobial peptide LL-37. *Stem Cells* 2010; 28: 2229-2238.

AJRCCM Articles in Press. Published April 15, 2020 as 10.1164/rccm.201911-2143OC

8. Jackson MV, Morrison TJ, Doherty DF, McAuley DF, Matthay MA, Kissenpfennig A, O'Kane CM, Krasnodembskaya AD. Mitochondrial Transfer via Tunneling Nanotubes is an Important Mechanism by Which Mesenchymal Stem Cells Enhance Macrophage Phagocytosis in the In Vitro and In Vivo Models of ARDS. *Stem Cells* 2016; 34: 2210-2223.

9. McIntyre LA, Moher D, Fergusson DA, Sullivan KJ, Mei SH, Lalu M, Marshall J, McLeod M, Griffin G, Grimshaw J, Turgeon A, Avey MT, Rudnicki MA, Jazi M, Fishman J, Stewart DJ, Canadian Critical Care Translational Biology G. Efficacy of Mesenchymal Stromal Cell Therapy for Acute Lung Injury in Preclinical Animal Models: A Systematic Review. *PLoS One* 2016; 11: e0147170.

10. Matthay MA, Calfee CS, Zhuo H, Thompson BT, Wilson JG, Levitt JE, Rogers AJ, Gotts JE, Wiener-Kronish JP, Bajwa EK, Donahoe MP, McVerry BJ, Ortiz LA, Exline M, Christman JW, Abbott J, Delucchi KL, Caballero L, McMillan M, McKenna DH, Liu KD. Treatment with allogeneic mesenchymal stromal cells for moderate to severe acute respiratory distress syndrome (START study): a randomised phase 2a safety trial. *Lancet Respir Med* 2018; 7(2):154-162.

11. Combes A, Hajage D, Capellier G, Demoule A, Lavoue S, Guervilly C, Da Silva D, Zafrani L, Tirot P, Veber B, Maury E, Levy B, Cohen Y, Richard C, Kalfon P, Bouadma L, Mehdaoui H, Beduneau G, Lebreton G, Brochard L, Ferguson ND, Fan E, Slutsky AS, Brodie D, Mercat A. Extracorporeal Membrane Oxygenation for Severe Acute Respiratory Distress Syndrome. *N Engl J Med*; 378: 1965-1975.

12. Hoogduijn MJ, van den Beukel JC, Wiersma LCM, Ijzer J. Morphology and size of stem cells from mouse and whale: observational study. *Br Med J* 2013; 347: f6833.

AJRCCM Articles in Press. Published April 15, 2020 as 10.1164/rccm.201911-2143OC

13. Dominici M, Le Blanc K, Mueller I, Slaper-Cortenbach I, Marini F, Krause D, Deans R, Keating A, Prockop D, Horwitz E. Minimal criteria for defining multipotent mesenchymal stromal cells. The International Society for Cellular Therapy position statement. *Cytotherapy* 2006; 8: 315-317.

14. Millar JE, von Bahr V, Malfertheiner MV, Ki KK, Redd MA, Bartnikowski N, Suen JY, McAuley DF, Fraser JF. Administration of mesenchymal stem cells during ECMO results in a rapid decline in oxygenator performance. *Thorax* 2018.

15. Cho HJ, Hong H, Kim DW, Lee KS, Han HS, Kim GH, Choi KS, Kim YS, Qayumov M, Ki KK, Suen J, Fraser J, Jeong IS. Viability of Mesenchymal Stem Cells in an Ex Vivo Circulation System. *ASAIO J* 2019. doi: 10.1097/MAT.0000000000001025. [Epub ahead of print].

16. Millar JE, Fanning JP, McDonald CI, McAuley DF, Fraser JF. The inflammatory response to extracorporeal membrane oxygenation (ECMO): a review of the pathophysiology. *Crit Care* 2016; 20: 387.

17. Council NHaMR. Australian code for the care and use of animals for scientific purposes. In: Council NHaMR, editor, 8th Edition ed. Canberra; 2013.

18. Kilkenny C, Browne WJ, Cuthill IC, Emerson M, Altman DG. Improving bioscience research reporting: the ARRIVE guidelines for reporting animal research. *Osteoarthr Cartilage* 2012; 20: 256-260.

19. Matute-Bello G, Downey G, Moore BB, Groshong SD, Matthay MA, Slutsky AS, Kuebler WM. An official American Thoracic Society workshop report: features and measurements of experimental acute lung injury in animals. *Am J Respir Cell Mol Biol* 2011; 44: 725-738.

AJRCCM Articles in Press. Published April 15, 2020 as 10.1164/rccm.201911-2143OC

20. Millar JE, Bartnikowski N, von Bahr V, Malfertheiner MV, Obonyo NG, Belliato M, Suen JY, Combes A, McAuley DF, Lorusso R, Fraser JF. Extracorporeal membrane oxygenation (ECMO) and the acute respiratory distress syndrome (ARDS): a systematic review of pre-clinical models. *Intensive Care Med Exp* 2019; 7: 18.

21. Griffiths MJD, McAuley DF, Perkins GD, Barrett N, Blackwood B, Boyle A, Chee N, Connolly B, Dark P, Finney S, Salam A, Silversides J, Tarmey N, Wise MP, Baudouin SV. Guidelines on the management of acute respiratory distress syndrome. *BMJ Open Respir Res* 2019; 6: e000420.

22. Simonson OE, Mougiakakos D, Heldring N, Bassi G, Johansson HJ, Dalen M, Jitschin R, Rodin S, Corbascio M, El Andaloussi S, Wiklander OP, Nordin JZ, Skog J, Romain C, Koestler T, Hellgren-Johansson L, Schiller P, Joachimsson PO, Hagglund H, Mattsson M, Lehtio J, Faridani OR, Sandberg R, Korsgren O, Krampera M, Weiss DJ, Grinnemo KH, Le Blanc K. In Vivo Effects of Mesenchymal Stromal Cells in Two Patients With Severe Acute Respiratory Distress Syndrome. *Stem Cells Tranl Med* 2016; 5: 845.

23. Lin H-C, Wang C-C, Chou H-W, Wu E-T, Lu FL, Ko B-S, Yao M, Wang P-Y, Wu M-H, Chen Y-S. Airway Delivery of Bone Marrow–Derived Mesenchymal Stem Cells Reverses Bronchopulmonary Dysplasia Superimposed with Acute Respiratory Distress Syndrome in an Infant. *Cell Med* 2018; 10: 2155179018759434.

24. Kocyildirim E, Cardenes N, Ting A, Caceres E, BermUdez C, Rojas M. The Use of GMP-Produced Bone Marrow-Derived Stem Cells in Combination with Extracorporeal Membrane Oxygenation in ARDS: An Animal Model. *ASAIO J* 2017; 63: 324-332.

25. McIntyre LA, Moher D, Fergusson DA, Sullivan KJ, Mei SH, Lalu M, Marshall J, McLeod M, Griffin G, Grimshaw J, Turgeon A, Avey MT, Rudnicki MA, Jazi M, Fishman J,

AJRCCM Articles in Press. Published April 15, 2020 as 10.1164/rccm.201911-2143OC

Stewart DJ. Efficacy of Mesenchymal Stromal Cell Therapy for Acute Lung Injury in Preclinical Animal Models: A Systematic Review. *PloS One* 2016; 11: e0147170.

26. Christy BA, Herzig MC, Montgomery RK, Delavan C, Bynum JA, Reddoch KM, Cap AP. Procoagulant activity of human mesenchymal stem cells. *J Trauma Acute Care Surg* 2017; 83: S164-s169.

27. Fiedler T, Rabe M, Mundkowski RG, Oehmcke-Hecht S, Peters K. Adipose-derived mesenchymal stem cells release microvesicles with procoagulant activity. *Int J Biochem Cell Biol* 2018; 100: 49-53.

28. Gleeson BM, Martin K, Ali MT, Kumar AH, Pillai MG, Kumar SP, O'Sullivan JF, Whelan D, Stocca A, Khider W, Barry FP, O'Brien T, Caplice NM. Bone Marrow-Derived Mesenchymal Stem Cells Have Innate Procoagulant Activity and Cause Microvascular Obstruction Following Intracoronary Delivery: Amelioration by Antithrombin Therapy. *Stem Cells* 2015; 33: 2726-2737.

29. Tatsumi K, Ohashi K, Matsubara Y, Kohori A, Ohno T, Kakidachi H, Horii A, Kanegae K, Utoh R, Iwata T, Okano T. Tissue factor triggers procoagulation in transplanted mesenchymal stem cells leading to thromboembolism. *Biochem Biophys Res Commun* 2013; 431: 203-209.

30. Curley GF, Hayes M, Ansari B, Shaw G, Ryan A, Barry F, O'Brien T, O'Toole D, Laffey JG. Mesenchymal stem cells enhance recovery and repair following ventilator-induced lung injury in the rat. *Thorax* 2012; 67: 496-501.

31. Pedrazza L, Cunha AA, Luft C, Nunes NK, Schimitz F, Gassen RB, Breda RV, Donadio MV, de Souza Wyse AT, Pitrez PMC, Rosa JL, de Oliveira JR. Mesenchymal stem cells improves survival in LPS-induced acute lung injury acting through inhibition of NETs formation. *J Cell Physiol* 2017; 232: 3552-3564.

AJRCCM Articles in Press. Published April 15, 2020 as 10.1164/rccm.201911-2143OC

32. Moodley Y, Sturm M, Shaw K, Shimbori C, Tan DB, Kolb M, Graham R. Human mesenchymal stem cells attenuate early damage in a ventilated pig model of acute lung injury. *Stem Cell Res* 2016; 17: 25-31.

33. Lalu MM, Sullivan KJ, Mei SH, Moher D, Straus A, Fergusson DA, Stewart DJ, Jazi M, MacLeod M, Winston B, Marshall J, Hutton B, Walley KR, McIntyre L. Evaluating mesenchymal stem cell therapy for sepsis with preclinical meta-analyses prior to initiating a first-in-human trial. *eLife* 2016; 5.

34. McIntyre LA, Stewart DJ, Mei SHJ, Courtman D, Watpool I, Granton J, Marshall J, Dos Santos C, Walley KR, Winston BW, Schlosser K, Fergusson DA. Cellular Immunotherapy for Septic Shock. A Phase I Clinical Trial. *Am J Crit Care Med* 2018; 197: 337-347.

35. Galstian GM, Parovichnikova EN, Makarova PM, Kuzmina LA, Troitskaya VV, Gemdzhian E, Drize NI, Savchenko VG. The Results of the Russian Clinical Trial of Mesenchymal Stromal Cells (MSCs) in Severe Neutropenic Patients (pts) with Septic Shock (SS) (RUMCESS trial). *Blood* 2015; 126: 2220.

36. Schlosser K, Wang J-P, Dos Santos C, Walley KR, Marshall J, Fergusson DA, Winston BW, Granton J, Watpool I, Stewart DJ, McIntyre LA, Mei SHJ, Canadian Critical Care Trials G, the Canadian Critical Care Translational Biology G. Effects of Mesenchymal Stem Cell Treatment on Systemic Cytokine Levels in a Phase 1 Dose Escalation Safety Trial of Septic Shock Patients. *Crit Care Med* 2019; 47: 918-925.

37. Perlee D, van Vught LA, Scicluna BP, Maag A, Lutter R, Kemper EM, van 't Veer C, Punchard MA, Gonzalez J, Richard MP, Dalemans W, Lombardo E, de Vos AF, van der Poll T. Intravenous Infusion of Human Adipose Mesenchymal Stem Cells Modifies

AJRCCM Articles in Press. Published April 15, 2020 as 10.1164/rccm.201911-2143OC

the Host Response to Lipopolysaccharide in Humans: A Randomized, Single-Blind, Parallel Group, Placebo Controlled Trial. *Stem Cells* 2018; 36(11):1778-1788.

38. Laroye C, Lemarié J, Boufenzer A, Labroca P, Cunat L, Alauzet C, Groubatch F, Cailac C, Jolly L, Bensoussan D, Reppel L, Gibot S. Clinical-grade mesenchymal stem cells derived from umbilical cord improve septic shock in pigs. *Intensive Care Med* 2018; 6: 24-24.

39. Laroye C, Boufenzer A, Jolly L, Cunat L, Alauzet C, Merlin JL, Yguel C, Bensoussan D, Reppel L, Gibot S. Bone marrow vs Wharton's jelly mesenchymal stem cells in experimental sepsis: a comparative study. *Stem Cell Res Ther* 2019; 10: 192.

40. Cardenes N, Aranda-Valderrama P, Carney JP, Sellares Torres J, Alvarez D, Kocydirim E, Wolfram Smith JA, Ting AE, Lagazzi L, Yu Z, Mason S, Santos E, Lopresti BJ, Rojas M. Cell therapy for ARDS: efficacy of endobronchial versus intravenous administration and biodistribution of MAPCs in a large animal model. *BMJ Open Respir Res* 2019; 6: e000308.

41. Matthay MA, Zemans RL, Zimmerman GA, Arabi YM, Beitler JR, Mercat A, Herridge M, Randolph AG, Calfee CS. Acute respiratory distress syndrome. *Nat Rev Dis Primers* 2019; 5: 18.

42. Islam D, Huang Y, Fanelli V, Delsedime L, Wu S, Khang J, Han B, Grassi A, Li M, Xu Y, Luo A, Wu J, Liu X, McKillop M, Medin J, Qiu H, Zhong N, Liu M, Laffey J, Li Y, Zhang H. Identification and Modulation of Microenvironment Is Crucial for Effective Mesenchymal Stromal Cell Therapy in Acute Lung Injury. *Am J Crit Care Med* 2018; 199: 1214-1224.

43. Cavalcanti AB, Suzumura EA, Laranjeira LN, Paisani DM, Damiani LP, Guimaraes HP, Romano ER, Regenga MM, Taniguchi LNT, Teixeira C, Pinheiro de Oliveira R,

AJRCCM Articles in Press. Published April 15, 2020 as 10.1164/rccm.201911-2143OC

Machado FR, Diaz-Quijano FA, Filho MSA, Maia IS, Caser EB, Filho WO, Borges MC, Martins PA, Matsui M, Ospina-Tascon GA, Giancursi TS, Giraldo-Ramirez ND, Vieira SRR, Assef M, Hasan MS, Szczeklik W, Rios F, Amato MBP, Berwanger O, Ribeiro de Carvalho CR. Effect of Lung Recruitment and Titrated Positive End-Expiratory Pressure (PEEP) vs Low PEEP on Mortality in Patients With Acute Respiratory Distress Syndrome: A Randomized Clinical Trial. *JAMA* 2017; 318: 1335-1345.

AJRCCM Articles in Press. Published April 15, 2020 as 10.1164/rccm.201911-2143OC

Figure Legends

Figure 1. Study schematic.

[a] Adjusted to maintain pH 7.30-7.45. Permissive hypercapnia was tolerated to a minimum pH of 7.15.

[b] PaO_2 55 – 80 mmHg. If despite an FiO_2 of 1.0 oxygenation targets were not met, PEEP was increased, maintaining plateau pressure ≤ 32 cmH_2O.

[c] Total PEEP (extrinsic PEEP + intrinsic PEEP) did not exceed 20 cmH_2O. PEEP was permitted to be reduced to 5 cmH_2O to maintain plateau pressure ≤ 30 cmH_2O. If despite a PEEP of 5 cmH_2O, plateau pressure > 30 cmH_2O, tidal volume was reduced in 1 mL/kg steps until set at 4 mL/kg.

Figure 2. Oxygenation and respiratory parameters.

a. PaO_2/FiO_2 ratio. **b.** Oxygenation index. **c.** Airway pressures and lung compliance. Data are presented as mean (± 95% confidence interval). Where error bars intersect the x axis the 95% CI includes zero.

Figure 3. Hemodynamic variables.

a. Mean arterial pressure and vasopressor dose (mean). **b.** Mean pulmonary artery pressure. **c.** Cumulative vasopressor dose. **d.** Cardiac index, base deficit, and arterial lactate. Data are presented as mean (± 95% confidence interval). Where error bars intersect the x axis the 95% CI includes zero. ** - $p < 0.01$.

Figure 4. Histopathology and lung injury.

a. Representative images of lung parenchyma. All animals showed evidence of diffuse alveolar damage however the frequency and degree of injury differed between groups. **Panel 1:** extensive alveolar edema with interstitial leukocyte infiltration. **Panel 2:** marked leukocyte infiltration within alveolar spaces and larger airways. **Panel 3:** some loss of alveolar structure with edema however a reduction in interstitial and alveolar leukocytes. **Panel 4:** preservation

AJRCCM Articles in Press. Published April 15, 2020 as 10.1164/rccm.201911-2143OC

of alveolar architecture with few leukocytes in the alveolar spaces. **Panel 5 & 6:** representative images of pulmonary arterial and arteriolar emboli (black arrows) in animals receiving hMCSs. **b.** Composite lung injury score (LIS), lung wet/dry ratio (right lower lobe). **c.** BAL total protein concentration. Data are presented as mean (± 95% confidence interval). * - p = < 0.05.

Figure 5. Cell-ECMO interaction.

a. Trans-membrane oxygenator pressure gradient. **b.** Pump revolutions per minute (RPM)/flow ratio. Data are presented as mean (± 95% confidence interval). Where error bars intersect the x axis the 95% CI includes zero. * - p = < 0.05.

AJRCCM Articles in Press. Published April 15, 2020 as 10.1164/rccm.201911-2143OC

Table 1. Baseline physiological characteristics

	Overall (n=14)	**Vehicle** (n=7)	**hMSCs** (n=7)
Weight (kg)	52.6 ± 3	52.4 ± 3.2	52.9 ± 2.6
Pre-ECMO tidal volume (mL/kg)	6.0 ± 0.1	6.0 ± 0.1	6.0 ± 0.1
At time of injury (T0)			
Peak airway pressure (cmH_2O)	31.5 ± 4.2	31.9 ± 3.3	31.1 ± 4.9
Plateau pressure (cmH_2O)	26.5 ± 3.9	26.1 ± 3.9	26.9 ± 3.8
Driving pressure (cmH_2O)	16.5 ± 3.9	16.1 ± 3.9	16.9 ± 3.8
Static compliance (mL/cmH_2O)	21 ± 5.0	19 ± 4.6	23 ± 4.6
PaO_2/FiO_2	59 ± 20	58 ± 23	61 ± 17
$PaCO_2$ (mmHg)	41 (38-46)	38 (38-41)	44 (41-48)
pH	7.36 ± 0.05	7.38 ± 0.04	7.34 ± 0.05
Bicarbonate (mmol/L)	23.2 ± 1.5	23.6 ± 1.4	22.9 ± 1.5
Base deficit (mmol/L)	1.30 ± 1.31	0.94 ± 1.15	1.66 ± 1.37
Arterial lactate (mmol/L)	1.6 ± 0.7	1.8 ± 0.6	1.4 ± 0.7
Heart rate (bpm)	102 (96-117)	108 (98-128)	98 (95-103)
Mean arterial pressure (mmHg)	103 ± 19	96 ± 16	111 ± 19
Central venous pressure (mmHg)	13 (11-13)	12 (11-13)	13 (13-14)
Mean pulmonary artery pressure (mmHg)	25 (16-29)	20 (17-27)	28 (19-29)

AJRCCM Articles in Press. Published April 15, 2020 as 10.1164/rccm.201911-2143OC

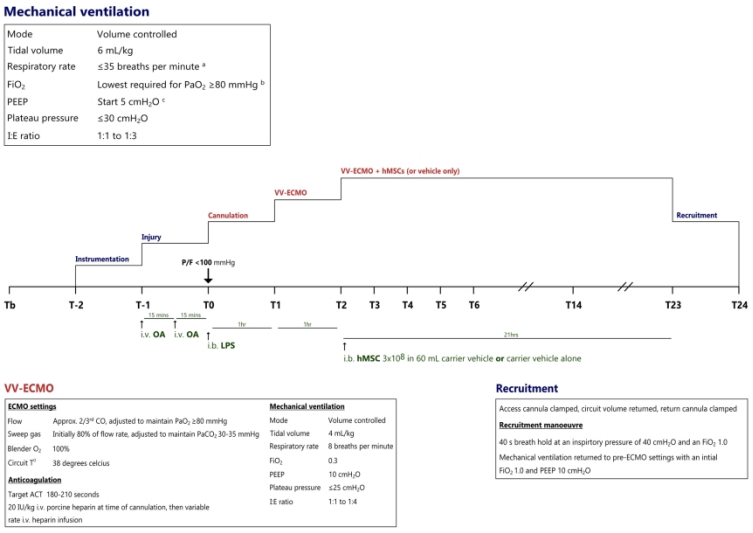

Figure 1

210x297mm (300 x 300 DPI)

AJRCCM Articles in Press. Published April 15, 2020 as 10.1164/rccm.201911-2143OC

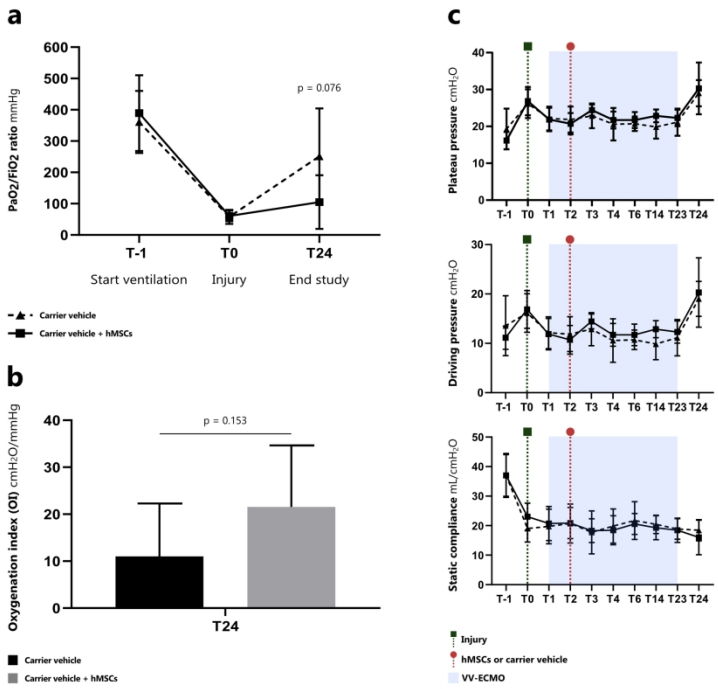

Figure 2

210x297mm (300 x 300 DPI)

AJRCCM Articles in Press. Published April 15, 2020 as 10.1164/rccm.201911-2143OC

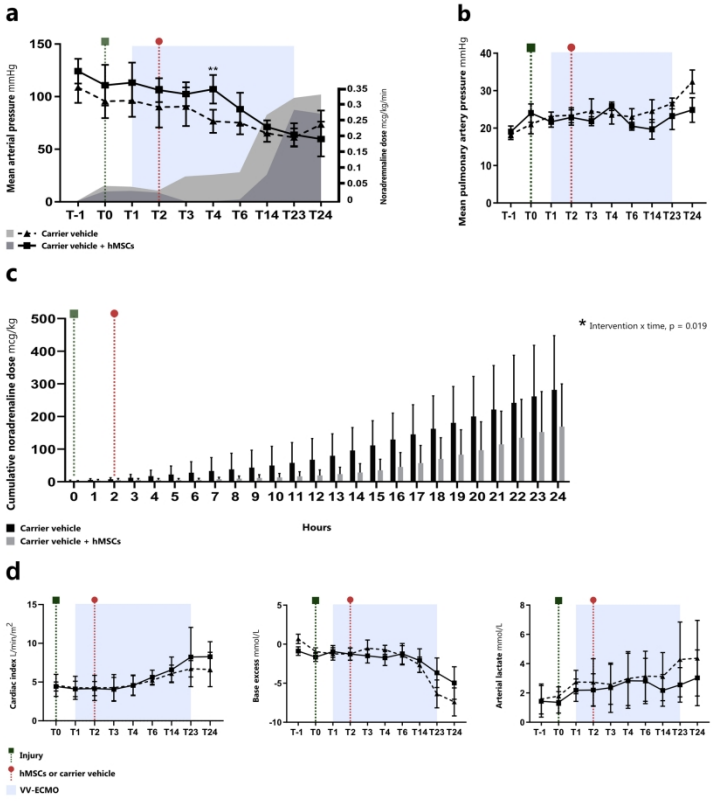

Figure 3

210x297mm (300 x 300 DPI)

AJRCCM Articles in Press. Published April 15, 2020 as 10.1164/rccm.201911-2143OC

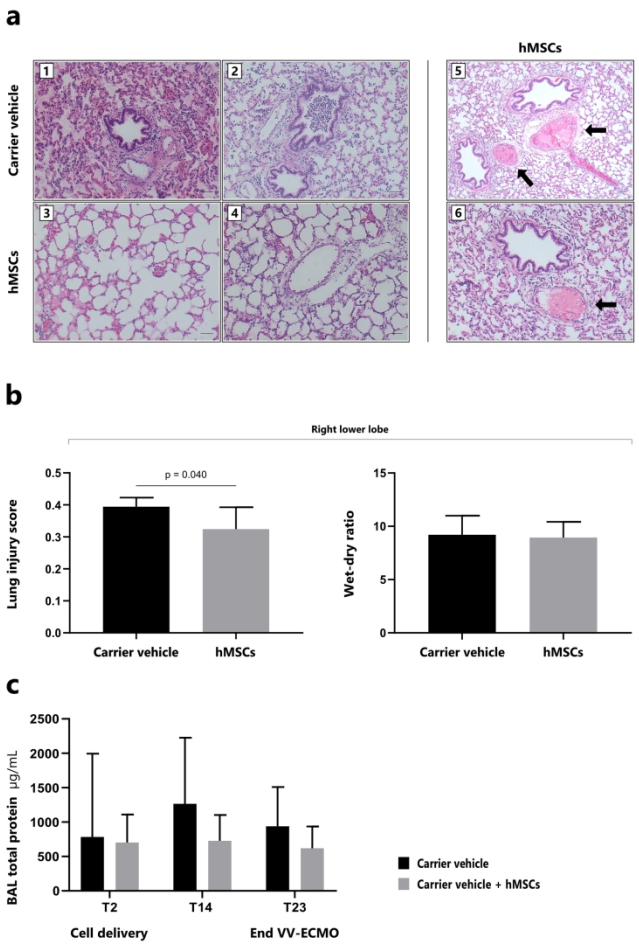

Figure 4

210x297mm (300 x 300 DPI)

AJRCCM Articles in Press. Published April 15, 2020 as 10.1164/rccm.201911-2143OC

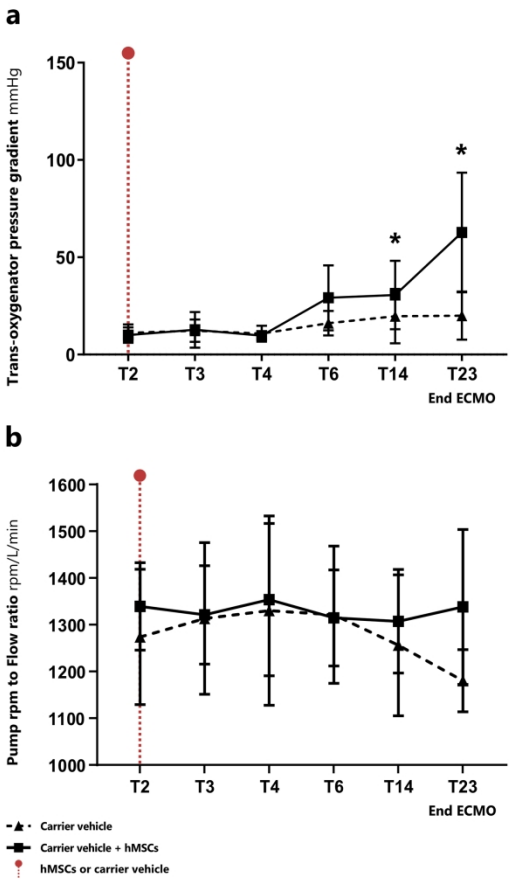

Figure 5

210x297mm (300 x 300 DPI)

AJRCCM Articles in Press. Published April 15, 2020 as 10.1164/rccm.201911-2143OC

Combined Mesenchymal Stromal Cell Therapy and ECMO in ARDS: A Controlled Experimental Study in Sheep

Jonathan E Millar, Nicole Bartnikowski, Margaret R Passmore, Nchafatso G Obonyo, Maximillian V Malfertheiner, Viktor von Bahr, Meredith A Redd, Louise See Hoe, Katrina K Ki, Sanne Pedersen, Andrew J Boyle, J Kenneth Baillie, Kiran Shekar, Nathan Palpant, Jacky Y Suen, Michael A Matthay, Daniel F McAuley, John F Fraser on behalf of the Combining Extracorporeal Life Support and Cell Therapy in Critical Illness (CELTIC) investigators

Online Supplement

Contents

AJRCCM Articles in Press. Published April 15, 2020 as 10.1164/rccm.201911-2143OC

A. Sheep preparation

Female sheep (*Ovis aries*, Border Leicester Cross), aged 1-3 years, were selected at random from a flock of healthy farm reared animals. Sheep were transferred to the animal research facility at least two weeks before use. They could graze freely in an outdoor enclosure and underwent veterinary inspection, including testing for common ovine pathogens (e.g. Q fever). On the day before experimentation, animals were housed in an indoor pen with free access to water and were denied solid feed for 12 hours. On the morning of experimentation, sheep were transported to the operating theatre in a specially modified sling.

Under local anesthesia (5-10 mL 2% lignocaine, Pfizer, Sydney, NSW, Australia), a quad-lumen central venous catheter (Arrow, Teleflex Medical Australia, Mascot, NSW, Australia) was inserted into the left external jugular vein (EJV), after which baseline blood samples were obtained. An 8 Fr percutaneous introducer sheath (Arrow, Teleflex Medical Australia, Mascot, NSW, Australia) was inserted cephalad to the central venous catheter in the left EJV. Two 8 Fr percutaneous introducer sheaths were then inserted, approximately 8 cm apart, in the right EJV. All lines were secured with 1-0 silk sutures. Once vascular access was secured, animals were pre-oxygenated for 3 minutes using a facemask and a Mapleson C anesthetic circuit set to deliver 15 L O_2 min^{-1}. General anesthesia was then induced as described below. Animals were transferred to an operating table and positioned supine. A surgical tracheostomy was performed, by midline longitudinal incision exposing the space between the $2^{nd}/3^{rd}$ tracheal rings. A size 9.0 Portex tracheostomy tube (Smith's Medical Australia, Sydney, NSW, Australia) was inserted, and positioning was confirmed using a flexible video bronchoscope (aScope™, Ambu, Ballerup, Denmark). Thereafter, the tracheostomy was suctioned hourly using an in-line suction catheter.

AJRCCM Articles in Press. Published April 15, 2020 as 10.1164/rccm.201911-2143OC

B. Supportive care protocol

Experienced medical and nursing staff, with training in the prevision of critical care and ECMO, were present for the duration of each experiment. Expert large animal veterinarian advice was available upon request.

Anesthesia/analgesia

General anesthesia was induced by intravenous injection of midazolam (0.5 mg/Kg, Pfizer, Sydney, NSW, Australia) and ketamine (5 mg/kg, Troy Laboratories, Sydney, NSW, Australia). Animals were orotracheally intubated (size 9.0-10.0 ID Portex endotracheal tube, Smith's Medical Australia, Sydney, NSW, Australia) and connected to a mechanical ventilator. Maintenance of anesthesia/analgesia was achieved by intravenous infusion of midazolam (0.5-0.8 mg/kg/hr, Pfizer, Sydney, NSW, Australia), ketamine (5-7.5 mg/kg/hr, Troy Laboratories, Sydney, NSW, Australia), and fentanyl (5-10 mcg/kg/hr, Hameln Pharmaceuticals, Hameln, Germany). Depth of anesthesia was assessed prior to neuromuscular blockade by abolition of the eyelash reflex, after which attention was paid to clinical indicators such as heart rate and salivation. Total intravenous anesthesia was maintained until euthanasia.

Once maintenance anesthesia was established, animals were paralysed with an intravenous bolus of vecuronium (50 mcg/kg, Pfizer, Sydney, NSW, Australia). Adequacy of neuromuscular blockade (NMB) was assessed using the train of four (TOF) response to peripheral nerve stimulation. NMB was maintained through the course of the experiment by an intravenous infusion of vecuronium (50 mcg/kg/hr, Pfizer, Sydney, NSW, Australia).

Mechanical ventilation

In the period between induction of anesthesia and the commencement of VV-ECMO, animals were ventilated according to a protocolized lung-protective strategy (**Table A**). In a volume-controlled mode, the ventilator was initially set to achieve a tidal volume (V_t) of 6

AJRCCM Articles in Press. Published April 15, 2020 as 10.1164/rccm.201911-2143OC

mL/kg actual body weight (ABW). One of, a Hamilton Galileo (Hamilton Medical, Bonaduz, Switzerland) or a Puritan Bennett 840 (Puritan Bennett, Medtronic, Dublin, Ireland) ventilator was used for the full course of each study.

Parameter	**Value**
Mode	Volume controlled
Tidal Volume (V_t)	4 - 6 mL/kg
Respiratory Rate	≤ 35 breaths per minute[a]
FiO_2	Lowest required for SpO_2 88-93%[b]
PEEP	Adjusted to maintain P_{plat} 28-30 cmH_2O[c]
Plateau Pressure (P_{plat})	≤ 30 cmH_2O
I:E Ratio	1:1 to 1:3

Table A. Pre-ECMO ventilatory strategy.

[a] Adjusted to maintain pH 7.30-7.45. Permissive hypercapnia was tolerated to a minimum pH of 7.15.

[b] PaO_2 55 – 80 mmHg. If despite an FiO_2 of 1.0 oxygenation targets were not met, PEEP was increased, maintaining P_{plat} ≤ 32 cmH_2O.

[c] Total PEEP (extrinsic PEEP + intrinsic PEEP) did not exceed 20 cmH_2O. PEEP was permitted to be reduced to 5 cmH_2O to maintain P_{plat} ≤ 30 cmH_2O. If despite a PEEP of 5 cmH_2O, P_{plat} > 30 cmH_2O, V_t was reduced in 1 mL/kg steps until set at 4 mL/kg.

FiO_2 – Fraction of inspired oxygen, SpO_2 – Peripheral oxygen saturation, PEEP – Positive end-expiratory pressure, P_{plat} – Airway plateau pressure, I:E Ratio – Inspiratory to expiratory ratio

Fluid and electrolyte management

After the induction of general anesthesia, a maintenance infusion of crystalloid (1-2 mL/kg/hr, compound sodium lactate, Baxter, Sydney, NSW, Australia) was commenced for

AJRCCM Articles in Press. Published April 15, 2020 as 10.1164/rccm.201911-2143OC

the duration of the study. Fluid therapy was indicated at other times to support hemodynamics or ECMO flows, in this case 100 mL boluses of compound sodium lactate were titrated to effect.

Electrolyte levels were assessed 4-hourly. Serum potassium levels were maintained > 3.5 mmol/L by i.v. infusion of 10-20 mmol potassium chloride (AstraZeneca, Sydney, NSW, Australia). In the event of hyperkalemia (K^+ > 5.5 mmol/L), supplemental potassium administration was ceased and 10 mL 10% calcium gluconate (B. Braun Melsungen AG, Melsungen, Germany) was given by i.v. bolus injection. Hyperchloremia (Cl^- >103) was avoided. All large volume gastric losses were returned via the orogastric tube. Blood glucose levels were measured hourly and maintained > 1.5 mmol/L by infusion of 50% glucose (Baxter, Sydney, NSW, Australia).

Monitoring and hemodynamic management

All animals were monitored according to the '*Recommendations for standards of monitoring during anaesthesia and recovery 2015: Association of Anaesthetists of Great Britain and Ireland*', including; pulse oximetry, 3-lead electrocardiogram, and continuous waveform capnography. In addition, the central venous catheter (CVC) was transduced as a measure of central venous pressure.

Following induction of general anesthesia and repositioning to the operating table, invasive arterial blood pressure monitoring was established by cannulation of the left facial artery (20G Leadercath arterial, Vygon, Écouen, France). Using the 8 Fr percutaneous sheath introducer positioned in the left EJV, a pulmonary artery catheter (PAC) was inserted (7.5 Fr Swan-Ganz CCOmbo, Edwards Life Sciences, Irvine, CA, USA). The catheter was inserted to a depth of 15 cm after which the flotation balloon was inflated. The catheter was directed to the pulmonary artery, the balloon was deflated, and the catheter secured. Positioning was

AJRCCM Articles in Press. Published April 15, 2020 as 10.1164/rccm.201911-2143OC

confirmed by obtaining a satisfactory waveform. Continuous cardiac output monitoring (Vigilance monitor, Edwards Lifesciences, Irvine, CA, USA) was instituted, with cardiac index estimated by; cardiac output/BSA [weight (kg)$^{0.67}$ x 0.0842]. Continuous measurements of core body temperature were also obtained from the PAC.

A 14 Fr urinary catheter (Gildana Healthcare, Oakleigh, VIC, Australia) was inserted and connected to an hourly urometer to allow for accurate quantification of urine output. A 16 Fr orogastric tube (ConvaTec, Glen Waverley, VIC, Australia) was inserted and left on free drainage.

A mean arterial pressure ≥ 65 mmHg was targeted. In the face of sustained hypotension, repeated 100 mL boluses of compound sodium lactate (Baxter, Sydney, NSW, Australia) were given until; CVP ≥ 8 mmHg and/or the animal was no longer fluid responsive (failure to increase stroke volume > 10% by PAC). Thereafter, noradrenaline (80 mcg/mL in 5% dextrose, Hospira, Lake Forrest, IL, USA) was commenced at 80 mcg/min and the dose titrated at 5-minute intervals. If noradrenaline requirements reached 2400 mcg/min, vasopressin (PPC, Richmond Hill, Canada) was commenced at 0.8 units/hr and increased to a maximum of 1.8 units/hr.

Euthanasia

At the end of each study, animals were euthanised by i.v. injection of phenobarbitone (142.5 mg/kg, Aspen Pharma, Dandenong, NSW, Australia). After death was confirmed (absence of cardiac electrical activity, blood pressure, and cardiac output monitoring), organs were retrieved surgically. Animal carcasses were stored and subsequently disposed of by incineration.

AJRCCM Articles in Press. Published April 15, 2020 as 10.1164/rccm.201911-2143OC

C. Model of experimental ARDS

After instrumentation, in a supine position, animals were injured using a combination of intravenous oleic acid (OA) and endobronchial *E. coli* lipopolysaccharide (LPS).

Oleic acid preparation

A total dose of 0.06 ml/kg OA was used to induce injury. Firstly, 0.03 mL/kg OA (O1008, Sigma-Aldrich, Castle Hill, NSW, Australia) was suspended in 20 mL arterial blood and 150 IU porcine heparin (Pfizer, Sydney, NSW, Australia). This mixture was administered via the distal port of the right EJV central venous catheter, followed by a flush of 50 mL 0.9% sodium chloride (Baxter, Sydney, NSW, Australia). The animal could recover and after 15 minutes this procedure was repeated. When 15 minutes elapsed from the second dose, arterial blood gas analysis, at an FiO_2 of 1.0 and a PEEP of 10 cmH_2O, was used to confirm a PaO_2/FiO_2 ratio <100 mmHg.

E. coli lipopolysaccharide preparation

Immediately after a PaO_2/FiO_2 ratio <100 mmHg was confirmed, 50 mcg *E. coli* LPS (O55:B5, Sigma-Aldrich, Castle Hill, NSW, Australia), diluted in 10 mL 0.9% sodium chloride (Baxter, Sydney, NSW, Australia), was administered, via a designated video bronchoscope, to each main bronchus.

AJRCCM Articles in Press. Published April 15, 2020 as 10.1164/rccm.201911-2143OC

D. Veno-venous ECMO

Equipment

ECMO was performed using a Maquet ROTAFLOW centrifugal pump (Maquet, Getinge Group, Rastatt, Germany) along with a Maquet Permanent Life Support (PLS) set (Maquet, Getinge Group, Rastatt, Germany). Circuits were primed in a sterile fashion (prime volume ~ 585 mL) with compound sodium lactate (Baxter, Sydney, NSW, Australia).

Cannulation

Cannulation attempts were commenced after injury was confirmed (T0). Two 19 Fr Bio-medicus single-stage venous catheters (Medtronic, Dublin, Ireland) were used in a right sided $V_{EJ} - V_{EJ}$ configuration. The access cannula was inserted by first re-wiring the proximal right EJV percutaneous sheath and was then positioned in the inferior vena cava at the level of the diaphragm. The return cannula was inserted by first re-wiring the distal right EJV percutaneous sheath and was then positioned with the tip at the cavo-atrial junction. Cannula insertion and positioning were guided by fluoroscopy and real-time intra-cardiac and intra-cannular echocardiography. Cannulae were flushed with heparinised 0.9% sodium chloride (10 IU/mL porcine heparin, Pfizer, NSW, Australia). Cannulae were secured by suturing to the skin. Animals were then placed in sternal recumbency for the remaining duration of the study.

Management

Once cannulation was successfully completed and positioning was confirmed, VV-ECMO was commenced (T1). Pump speeds were slowly increased to 1000 rpm before clamp release. Pump speeds were then adjusted to achieve flow rates of ~2/3 CO (typically between 60-90 mL/kg). Fresh gas flow (FGF) was initially set at 80% of pump flow and adjusted based on arterial blood gas analysis. The FGF blender was set to deliver 100% O_2 at all times. During ECMO, PaO_2 will be maintained $\geq$ 65 mmHg and $PaCO_2 \leq$ 45 mmHg. Hyperoxia (PaO_2 > 150

AJRCCM Articles in Press. Published April 15, 2020 as 10.1164/rccm.201911-2143OC

mmHg) will be avoided. A water heater-cooler unit was connected to the membrane oxygenator and set to 38° C for the duration of the ECMO run.

At the beginning of VV-ECMO, animals received a bolus dose of unfractionated heparin (20 IU/kg porcine heparin, Pfizer, Sydney, NSW, Australia), when the activated clotting time (ACT) fell below 160 s an infusion was commenced at 4 IU/kg/hr. An ACT of 180 s-210 s was targeted. ACT was measured prior to ECMO, at 1 hour, 2 hours, and every 2 hours thereafter. The unfractionated heparin infusion was titrated as per a pre-defined protocol (**Table B**).

ACT	**Response**
< 130	Bolus 10 IU/kg and increase infusion by 1.5 IU/kg/hr
130 - 150	Increase infusion by 1 IU/kg/hr
150 - 180	Increase infusion by 0.5 IU/kg/hr
180 - 210	No change
210 – 250	Decrease infusion by 1 IU/kg/hr
> 250	Cease infusion for 1 hr and recheck ACT, restart when ACT < 210 AND decrease infusion by 1.5 IU/kg/hr

Table B. ECMO anti-coagulation titration protocol.

Mechanical ventilation during ECMO

Once VV-ECMO was established, mechanical ventilation was adjusted to target an ultra-protective ventilatory strategy, consistent with that described in the EOLIA trial (1). Neuromuscular blockade was maintained throughout. Ventilator settings and targets are detailed further in **Table C**.

AJRCCM Articles in Press. Published April 15, 2020 as 10.1164/rccm.201911-2143OC

Termination and return to pre-ECMO mechanical ventilation

VV-ECMO was halted 23 hours after injury (T23). Pump speeds were gradually reduced to zero and both cannulae were clamped. Pump blood was returned by unclamping the return cannula and gently flushing the circuit with Compound Sodium Lactate (~585 mL blood returned). Clamped cannulae were left in situ until termination of the study. Immediately before cessation of VV-ECMO, a standardised recruitment manoeuvre was performed. The recruitment manoeuvre involved a 40 s breath hold at an airway pressure of 40 cmH_20, in a pressure-controlled mode, with an FiO_2 of 1.0. After which animals were returned to standardised pre-ECMO ventilator settings (with an FiO_2 of 1.0) for 60 minutes at which time the trial was terminated.

Parameter	**Value**
Mode	Volume controlled
Tidal Volume	≤ 4 ml/kg
Respiratory Rate	8 breaths per minute
FiO_2	0.30
PEEP	≥ 10 cmH_2O
Pplat	≤ 25 cmH_2O
I:E Ratio	1:1 to 1:3

Table C. ECMO ventilatory strategy.

AJRCCM Articles in Press. Published April 15, 2020 as 10.1164/rccm.201911-2143OC

E. Human mesenchymal stromal cells

Induced pluripotent stem cell (iPSC) derived human mesenchymal stromal cells (hMSCs) were obtained from Cynata Therapeutics Ltd. (CYP-001; Cynata Therapeutics Ltd., Melbourne, VIC, Australia). Cells were manufactured under Good Manufacturing Practices (GMP) conditions and were > 99% positive for CD-73, CD-90, and CD-105, but negative for CD-31 and CD-45. iPSC-derived hMSCs were between passage 3 and 5. iPSC derived hMSCs were presented in discrete batches of 1 x 10^8 cells, suspended in 20 mL of a carrier vehicle (57.5% Plasmalyte-A, 40% Flexbumin 25%, 2.5% Dimethyl sulfoxide). Cells were shipped to our laboratory stored in the vapour phase of liquid nitrogen at -80°C where this was maintained until use.

Cell preparation

Two hours before administration, cryopreserved cells in their carrier vehicle were thawed in a water bath at 37.5°C, agitated to prevent clumping, and decanted into a sterile container. Batches were sampled and assessed for viability (> 95%) prior to use.

Cell administration

Animals allocated to the treatment group received a fixed endobronchial dose of 3 x 10^8 cells (suspended in 60 mL of carrier vehicle), via a flexible video bronchoscope (aScope™, Ambu, Ballerup, Denmark). Those allocated to the control group, received an equal volume of cell-free carrier vehicle, administered in an identical fashion. Common to both groups, 25 mL of solution was administered to the left diaphragmatic lobar bronchus and 5 mL to the left apico-cardiac lobar bronchus, with a further 25 mL administered via the right diaphragmatic lobar bronchus and 5 mL via the right cardiac lobar bronchus. The right apical lobar bronchus, which arises in sheep directly from the trachea at approximately the level of the third rib (2),

AJRCCM Articles in Press. Published April 15, 2020 as 10.1164/rccm.201911-2143OC

was untreated. After each instance of cell delivery, the channel of the bronchoscope was flushed with 5 mL of 0.9% sodium chloride (Baxter, Sydney, NSW, Australia).

AJRCCM Articles in Press. Published April 15, 2020 as 10.1164/rccm.201911-2143OC

F. Clinical measurements

Hemodynamic and ventilatory data (including data derived from the PAC) were continuously monitored and automatically recorded at 5-minute intervals using a data monitoring system (Solar 8000, GE Healthcare, Waukesha, WI, USA) coupled with custom software. Pressure readings across the membrane oxygenator were made using a silicone-based pressure transducer (Omega Engineering, Norwalk, CT, USA), these data were recorded continuously using LabVIEW software (National Instruments, Austin, TX, USA). ECMO flow readings and pump revolutions were read and recorded on an hourly basis from the ROTAFLOW console (Maquet, Getinge Group, Rastatt, Germany). Urine and oro-gastric outputs were recorded on a pre-piloted observation chart on an hourly basis, while continuous temperature data were taken from the PAC.

AJRCCM Articles in Press. Published April 15, 2020 as 10.1164/rccm.201911-2143OC

G. Blood and bronchoalveolar lavage fluid analyses

Blood

Whole blood was sampled from the facial artery catheter. Arterial blood gas analysis was undertaken on at least an hourly basis (ABL800 FLEX, Radiometer, Copenhagen, Denmark). At baseline, T_{-1}, T_0, T_{1-4}, T_6, T_{14}, T_{23}, and T_{24}, blood was sampled for routine laboratory hematological and biochemical testing. These tests were undertaken in a blinded fashion by an accredited veterinary pathology laboratory (IDEXX Laboratories Pty. Ltd., Brisbane, QLD, Australia). At baseline, T_{-1}, T_0, T_{1-4}, T_6, T_{14}, T_{23}, and T_{24}, blood was sampled for plasma cytokine measurements. The concentration of IL-6, IL-1β, IL-8 and IL-10 in plasma and bronchoalveolar lavage (BAL) fluid was quantified by in-house ELISAs using methods published previously (3-5). Positive internal controls were used to ensure that inter- and intra-plate variability was < 10% and confirm the precision and accuracy of all ELISA assays.

Bronchoalveolar lavage fluid

BAL was undertaken by an experienced bronchoscopist using a video bronchoscope (aScope™, Ambu, Ballerup, Denmark). At each examination the right and left middle and lower lobes were sampled. Each lobe was injected with 20 mL sterile 0.9% sodium chloride (Baxter, Sydney, NSW, Australia) and gentle suction was applied. The lavage fluid was collected in a sterile universal container. BAL fluid was centrifuged, and the supernatant collected for ELISA analysis. Aliquots were also cytospun onto slides for inflammatory cell counts.

AJRCCM Articles in Press. Published April 15, 2020 as 10.1164/rccm.201911-2143OC

H. Histological analyses and lung tissue gene expression

After the confirmation of death, the heart and lungs were retrieved enbloc via a midline sternotomy. Lung tissue was set on ice and portions of left and right lower and upper lobe lung tissue were fixed in 10% buffered formalin for at least 24 hours, processed and embedded in paraffin. All sections (5 μm) were stained with haematoxylin and eosin. Sections were examined by an independent, blinded, veterinary pathologist and scored for features of lung injury (6).

Total RNA was isolated from lung tissue using the Invitrogen PureLink® RNA Mini Kit (Thermo Fisher Scientific, VIC, Australia). All samples were DNase treated (Invitrogen DNA-free™ DNA Removal kit; Thermo Fisher Scientific) and the concentration of RNA determined using a NanoDrop ND-1000 spectrophotometer (NanoDrop Technologies, DE, USA). First strand cDNA was synthesized from 1μg of RNA (iScript™ Select cDNA Synthesis kit; Bio-Rad, NSW, Australia).

A non-exhaustive panel of genes associated with epithelial, endothelial, and coagulative function were analysed. These genes have been associated with dysfunction in ARDS. In addition, a panel of matrix metalloproteinase genes and their regulators were analysed. Real-time Quantitative PCR was performed using primers for MMP1, MMP2, MMP7, TIMP1, TIMP2, AGER, VEGFA, ANGPT2, F3, vWF and SFTPD (PrimerDesign, Southampton, UK) with PrecisionFAST qPCR SYBR Green Master Mix with low ROX (Primer Design). Reactions consisted of 10 μL SYBR Green Master Mix, 1 μL mixed primers (300 nM), and 5 μL of cDNA (equivalent to 50 ng) and nuclease free water to a final volume of 20 μL. The cycling conditions were as follows: cDNA was denatured at 95°C for 2 min, followed by 40 cycles of 95°C for 5 s and 60°C for 20 s. Melt curve analysis was programmed at the end of the run, 60–90°C with increments rising by 0.5°C each step and a 5 s hold at each degree to

AJRCCM Articles in Press. Published April 15, 2020 as 10.1164/rccm.201911-2143OC

determine reaction specificity and the absence of contamination, mispriming and primer dimer. A no-template control was included for each primer set. An ovine specific SYBR Green reference gene assay (Primer Design) was used to evaluate the stability of six candidate normalization genes (GAPDH, RPL19, β-2M, ACTB, RPS26, YWHAZ) using real-time quantitative PCR. The Qbase PLUS program was used to identify the most stably expressed housekeeping genes and all data was subsequently normalized to geomean of GAPDH and RPL19.

Gene Symbol	Gene Name	Forward primer (5'→3')	Reverse primer (5'→3')	Amplicon size (bp)	PCR Efficiency[a]
MMP1	Matrix metallopeptidase 1	CGTGACTCAGTTTGTTCTTACTCC	GTGTGACATTGCTCCAGAGTTG	149	1.99
MMP2	Matrix metallopeptidase 2	ACAAATTCTGGAGATACAATGAGGT	CAGGTCCACCACAGCATCC	113	1.95
MMP7	Matrix metallopeptidase 7	TCCCAACCAGAATTAAAGAACACTG	GGAGACGCATAGATGAGTAAGACA	147	1.99
TIMP1	Tissue inhibitor of metallopeptidase 1	GCCTTATACCAGCGTTATGAGAT	GCAGGGGTGTAGATGAATCG	98	1.96
TIMP2	Tissue inhibitor of metallopeptidase 2	GGACTCTGGCAACGACATCTA	CTGGTCAGGTCCCTTGAACAT	88	1.99
AGER	Advanced glycosylation end-product specific receptor	CCAGCCCAGTTCTCCTCTGTA	GGCAGGTGTTTACTCATCACTTTC	98	2.00
VEGFA	Vascular endothelial growth factor A	TCACCAGGAAAGACTGACACAG	CTGGATTCAGGATTGTTCTGTCG	93	1.94
ANGPT2	Angiopoietin 2	GCACATAGTTCAACTTCGGTCAA	TGCTGCTTTTGGAGAACTGAATTA	141	1.91

AJRCCM Articles in Press. Published April 15, 2020 as 10.1164/rccm.201911-2143OC

Gene Symbol	Gene Name	Forward primer (5'→3')	Reverse primer (5'→3')	Amplicon size (bp)	PCR Efficiency[a]
F3	Coagulation factor III, tissue factor	AAGCCAGATTATCTAAGGAAAGACAAA	AGTCCACCCAGTTTCACCTTAC	125	1.93
vWF	von Willebrand factor	GGAGGTGAAGCACAGTGGC	CCAGGTAAGGGACAGAGACCA	89	2.11
SFTPD	Surfactant protein D	CCTCCATGTCTACCAACCATCG	CTGAGCAGCCAGGAAGATAAGAA	109	2.08

Table D. Primers used in qPCR analysis.

[a] PCR efficiencies were determined using the formula $10^{-1/slope}$

AJRCCM Articles in Press. Published April 15, 2020 as 10.1164/rccm.201911-2143OC

I. Analyses of membrane oxygenators

At the cessation of VV-ECMO (T_{23}) the circuit was disassembled and the membrane oxygenator (MO) was recovered. The MO was rinsed with 0.9% sodium chloride (Baxter, Sydney, NSW, Australia) until the effluent was observed to be clear, after which the MO was infused with 500 mL formaldehyde and then sealed. MOs were stored at 5° C overnight and then opened using a commercially available band saw. The fiber bundle was extracted, and approximate 5 cm x 5 cm sections were taken from the heat and gas exchange sections. These were stored in sterile containers in Phosphate Buffered Saline (PBS) until they were analyzed.

For immunohistochemical detection of MSCs, approximately 1 cm x 1 cm fiber sections were blocked for 3 hours in 2% HISS (heat inactivated sheep serum) and 0.5% triton X-100 in PBS. The samples were washed 3 times in PBS for 5 minutes each, followed by overnight incubation with primary antibodies at 4°C. After primary incubation, the fiber sections were washed 3 times in PBS for 5 minutes each, incubated in secondary antibody solution for 1 hour at room temperature, and then washed an additional 3 times in PBS for 5 minutes each. Primary antibodies: mouse Ab to CD105-FITC (ab18278, 1:10), rabbit Ab to CD73 (ab175396, 1:50), goat Ab to CD90 (ab189367, 1:100). Secondary antibodies: donkey anti-mouse 488 (Invitrogen, 1:100), donkey anti-rabbit 647 (Invitrogen, 1:100), donkey anti-goat 568 (Invitrogen, 1:100). Nuclei were counterstained with 1 μg/mL DAPI (4′,6-diamidino-2-phenylindole, Sigma-Aldrich, NSW, Australia) during secondary incubation. All antibodies were diluted in blocking solution during primary and secondary incubations. A widefield Nikon deconvolution microscope was used to acquire images using both 4X and 20X objectives. Final images were processed with ImageJ software.

AJRCCM Articles in Press. Published April 15, 2020 as 10.1164/rccm.201911-2143OC

J. Sample size calculation

Prior to the study commencing, a sample size calculation was undertaken based on a primary outcome of improvement in PaO_2/FiO_2 ratio. Using data from two previous trials of MSCs in ovine models of ARDS (7, 8), we calculated that 7 animals per group were required to detect a 100 mmHg difference in PaO_2/FiO_2 ratio (alpha 0.05, power 0.9, outcome SD 42 mmHg, paired test).

AJRCCM Articles in Press. Published April 15, 2020 as 10.1164/rccm.201911-2143OC

J. Results supplement

	Overall (n=14)	**Carrier vehicle** (n=7)	**hMSCs** (n=7)
At time of injury (T0)			
Haemoglobin (g/L)	106.7 ± 8.3	112.6 ± 7.1	100.9 ± 4.3
Haematocrit	0.322 ± 0.030	0.339 ± 0.032	0.306 ± 0.010
White cell count (x10^9/L)	1.8 (1.0-2.3)	1.6 (1.0-2.1)	2.0 (1.1-3.0)
Neutrophil count (x10^9/L)	0.4 (0.2-0.9)	0.3 (0.2-0.4)	0.9 (0.2-1.4)
Lymphocyte count (x10^9/L)	1.1 (0.9-1.4)	1.1 (0.8-1.3)	1.0 (0.9-1.5)
Monocyte count (x10^9/L)	0.1 (0-0.2)	0.2 (0.1-0.3)	0.1 (0-0.1)
Prothrombin time (s)	15.3 ± 1.6	16.3 ± 1.3	14.5 ± 1.3
Activated partial thromboplastin time (s)	24.6 ± 2.5	24.0 ± 3.0	25.2 ± 2.0
Sodium (mmol/L)	139 ± 3	140 ± 2	137 ± 3
Potassium (mmol/L)	3.6 (3.3-3.9)	3.6 (3.3-4.0)	3.5 (3.4-3.8)
Chloride (mmol/L)	106 (105-106)	106 (105-107)	105 (103-106)
Urea (mmol/L)	5.7 ± 1.1	5.9 ± 1.0	5.5 ± 1.3
Creatinine (mmol/L)	0.07 (0.06-0.07)	0.07 (0.06-0.07)	0.06 (0.06-0.07)
Albumin (g/L)	26 ± 2	26 ± 2	27 ± 2
Bilirubin (μmol/L)	3 (1-4)	3 (3-5)	1 (1-3)
Alkaline phosphatase (IU/L)	102 ± 26	89 ± 22	114 ± 23
Aspartate aminotransferase (IU/L)	83 (72-97)	82 (72-95)	84 (73-103)
Creatinine kinase (IU/L)	205 (205-242)	242 (200-299)	191 (162-255)

Supplementary Table E1. Baseline hematological and biochemical characteristics.

AJRCCM Articles in Press. Published April 15, 2020 as 10.1164/rccm.201911-2143OC

	Overall (n=14)	Carrier vehicle (n=7)	hMSCs (n=7)	P value*
Haemoglobin (g/L)	78.9 ± 14.1	78.6 ± 18.0	79.3 ± 7.1	0.930
Haematocrit	0.249 ± 0.040	0.247 ± 0.050	0.252 ± 0.023	0.855
White cell count (x10^9/L)	1.1 (0.8-1.4)	1.1 (0.9-2.2)	1.2 (0.7-1.3)	0.606
Neutrophil count (x10^9/L)	0.2 (0.2-0.5)	0.2 (0.2-0.9)	0.4 (0.1-0.5)	0.494
Lymphocyte count (x10^9/L)	0.7 ± 0.3	0.8 ± 0.4	0.6 ± 0.2	0.243
Monocyte count (x10^9/L)	0.1 (0.1-0.3)	0.1 (0.1-0.3)	0.2 (0.1-0.2)	0.779
Prothrombin time (s)	28.3 ± 5.7	27.8 ± 5.3	29.1 ± 6.3	0.755
Activated partial thromboplastin time (s)	45.5 ± 7.0	44.3 ± 7.9	47.8 ± 4.3	0.482
Sodium (mmol/L)	140 (137-141)	141 (138-142)	140 (136-141)	0.331
Potassium (mmol/L)	4.4 ± 0.7	4.4 ± 0.6	4.3 ± 0.7	0.857
Chloride (mmol/L)	111 (109-112)	112 (110-113)	111 (109-112)	0.331
Urea (mmol/L)	4.5 ± 1.2	4.7 ± 1.5	4.2 ± 0.8	0.493
Creatinine (mmol/L)	0.11 ± 0.03	0.11 ± 0.02	0.11 ± 0.03	0.654
Albumin (g/L)	16 ± 2	16 ± 2	15 ± 2	0.355
Bilirubin (μmol/L)	18 ± 5	19 ± 6	17 ± 4	0.436
Alkaline phosphatase (IU/L)	54 ± 15	56 ± 20	53 ± 8	0.735
Aspartate aminotransferase (IU/L)	171 (144-207)	200 (155-247)	143 (138-196)	0.259
Creatinine kinase (IU/L)	7498 ± 4079	8990 ± 4233	6006 ± 3303	0.482

Supplementary Table E2. Hematological and biochemical characteristics at the end of ECMO (T_{23}).

* P values corrected for multiple comparison.

AJRCCM Articles in Press. Published April 15, 2020 as 10.1164/rccm.201911-2143OC

	Overall (n=14)	**Carrier vehicle** (n=7)	**hMSCs** (n=7)	**P value***
Haemoglobin (g/L)	87.5 ± 13.6	86.0 ± 12.8	89.0 ± 14.2	0.733
Haematocrit	0.268 ± 0.040	0.265 ± 0.039	0.270 ± 0.041	0.846
White cell count (x10^9/L)	1.2 (1.0-1.6)	1.6 (1.1-2.0)	1.2 (0.9-1.3)	0.266
Neutrophil count (x10^9/L)	0.4 (0.1-0.6)	0.4 (0.2-0.8)	0.4 (0.1-0.6)	0.381
Lymphocyte count (x10^9/L)	0.7 (0.7-1.0)	1.0 (0.8-1.1)	0.7 (0.6-0.7)	0.047
Monocyte count (x10^9/L)	0.1 (0.1-0.1)	0.2 (0-0.3)	0.1 (0.1-0.1)	0.433
Prothrombin time (s)	29.5 ± 5.0	31.5 ± 5.9	27.9 ± 3.3	0.346
Activated partial thromboplastin time (s)	47.3 ± 4.5	47.7 ± 3.3	47.0 ± 5.2	0.831
Sodium (mmol/L)	139 (138-141)	140 (138-142)	139 (135-140)	0.139
Potassium (mmol/L)	4.4 ± 0.5	4.5 ± 0.5	4.4 ± 0.6	0.886
Chloride (mmol/L)	111 ± 4	112 ± 5	110 ± 2	0.392
Urea (mmol/L)	4.3 ± 1.0	4.4 ± 1.2	4.2 ± 0.8	0.839
Creatinine (mmol/L)	0.11 ± 0.03	0.11 ± 0.02	0.11 ± 0.03	0.656
Albumin (g/L)	17 ± 2	17 ± 2	17 ± 1	0.896
Bilirubin (μmol/L)	19 ± 8	19 ± 9	18 ± 7	0.960
Alkaline phosphatase (IU/L)	57 ± 18	53 ± 24	58 ± 10	0.992
Aspartate aminotransferase (IU/L)	190 (162-222)	185 (164-217)	191 (161-221)	0.931
Creatinine kinase (IU/L)	8008 ± 3351	8858 ± 2734	7157 ± 3679	0.415

Supplementary Table E3. Hematological and biochemical characteristics at T_{24}.

* P values corrected for multiple comparison.

AJRCCM Articles in Press. Published April 15, 2020 as 10.1164/rccm.201911-2143OC

	Carrier vehicle (n=7)	**hMSCs** (n=7)	**P value***
BAL Monocytes/macrophages (n/200 cells ± SD)			
T-1	194 ± 4	193 ± 5	0.005
T0	189 ± 8	186 ± 10	
T2	148 ± 37	163 ± 13	
T3	100 ± 54	118 ± 36	
T4	38 ± 28	74 ± 52	
T6	33 ± 26	37 ± 28	
T14	37 ± 38	14 ± 13	
T23	21 ± 10	11 ± 12	
BAL Neutrophils (n/200 cells ± SD)			
T-1	4 ± 4	6 ± 5	0.008
T0	9 ± 6	12 ± 9	
T2	51 ± 37	36 ± 9	
T3	96 ± 54	80 ± 34	
T4	156 ± 29	123 ± 51	
T6	162 ± 26	158 ± 28	
T14	160 ± 37	184 ± 13	
T23	178 ± 11	186 ± 13	
BAL Lymphocytes (n/200 cells ± SD)			
T-1	2 ± 2	1 ± 1	0.169
T0	2 ± 6	2 ± 3	
T2	1 ± 1	1 ± 1	
T3	2 ± 3	0 ± 1	
T4	2 ± 2	1 ± 1	
T6	2 ± 3	0 ± 1	
T14	1 ± 1	1 ± 1	
T23	0 ± 1	2 ± 2	
BAL Eosinophils (n/200 cells ± SD)			
T-1	0 ± 0	0 ± 0	0.295
T0	0 ± 1	0 ± 1	
T2	1 ± 1	1 ± 2	
T3	2 ± 3	2 ± 2	
T4	4 ± 4	2 ± 2	
T6	3 ± 4	1 ± 2	
T14	3 ± 3	1 ± 1	
T23	2 ± 2	1 ± 1	

Supplementary Table E4. Bronchoalveolar lavage fluid cell counts.

Pooled BAL from right and left lower lobes. Two hundred cells per count. * P values presented for mixed model group:time interaction.

AJRCCM Articles in Press. Published April 15, 2020 as 10.1164/rccm.201911-2143OC

Figure E1. Bronchoscopic hMSC delivery

Volumes of carrier fluid instilled and location of delivery within the ovine pulmonary tree.

Figure E2. ECMO management

a. ECMO system variables and gas exchange on ECMO. Points represent individual observations. Dashed lines represent lower (PaO_2) and upper ($PaCO_2$) targets. **b.** Anticoagulation during ECMO. Activated partial thromboplastin time (APTT) ratio and heparin dose are presented as mean (± 95% confidence interval).

Figure E3. Lung tissue qPCR

a. Matrix metalloproteinases (MMPs) and inhibitors (TIMPS). **b.** Tissue factor (F3). **c.** Epithelial markers. AGER – receptor for advanced glycation endpoints, SPFTD – surfactant protein D. **d.** Endothelial markers. ANGPT2 – angiopoietin-2, VEGFA – vascular endothelial growth factor A, vWF – von Willebrand factor. Results are presented as mean (± 95% confidence interval).

Figure E4. Bronchoalveolar lavage fluid cytokines

Data presented as mean (± 95% confidence interval). Where error bars intersect the x axis the 95% CI includes zero. * - $p < 0.05$.

Figure E5. Plasma cytokines and leukocytes

a. Plasma cytokine concentrations. **b.** Leukocyte counts in whole blood. Data presented as mean (± 95% confidence interval). Where error bars intersect the x axis the 95% CI includes zero. . * - $p < 0.05$.

Figure E6. Immunofluorescence of explanted oxygenator fibers.

DAPI - 4′,6-diamidino-2-phenylindole.

AJRCCM Articles in Press. Published April 15, 2020 as 10.1164/rccm.201911-2143OC

K. Supplement references

E1. Combes A, Hajage D, Capellier G, Demoule A, Lavoue S, Guervilly C, Da Silva D, Zafrani L, Tirot P, Veber B, Maury E, Levy B, Cohen Y, Richard C, Kalfon P, Bouadma L, Mehdaoui H, Beduneau G, Lebreton G, Brochard L, Ferguson ND, Fan E, Slutsky AS, Brodie D, Mercat A. Extracorporeal Membrane Oxygenation for Severe Acute Respiratory Distress Syndrome. *N Engl J Med* 2018; 378: 1965-1975.

2. Hare WC. The broncho-pulmonary segments in the sheep. *J Anat* 1955; 89: 387-402.

3. Dooley LM, Abdalmula A, Washington EA, Kaufman C, Tudor EM, Ghosh P, Itescu S, Kimpton WG, Bailey SR. Effect of mesenchymal precursor cells on the systemic inflammatory response and endothelial dysfunction in an ovine model of collagen-induced arthritis. *PloS one* 2015; 10: e0124144.

4. Herndon CN, Foreyt WJ, Srikumaran S. Differential expression of interleukin-8 by polymorphonuclear leukocytes of two closely related species, Ovis canadensis and Ovis aries, in response to Mannheimia haemolytica infection. *Infect Immun* 2010; 78: 3578-3584.

5. Karisnan K, Bakker AJ, Song Y, Noble PB, Pillow JJ, Pinniger GJ. Interleukin-1 receptor antagonist protects against lipopolysaccharide induced diaphragm weakness in preterm lambs. *PloS one* 2015; 10: e0124390.

6. Matute-Bello G, Downey G, Moore BB, Groshong SD, Matthay MA, Slutsky AS, Kuebler WM. An official American Thoracic Society workshop report: features and measurements of experimental acute lung injury in animals. *Am J Resp Cell Mol* 2011; 44: 725-738.

7. Asmussen S, Ito H, Traber DL, Lee JW, Cox RA, Hawkins HK, McAuley DF, McKenna DH, Traber LD, Zhuo H, Wilson J, Herndon DN, Prough DS, Liu KD, Matthay MA,

AJRCCM Articles in Press. Published April 15, 2020 as 10.1164/rccm.201911-2143OC

Enkhbaatar P. Human mesenchymal stem cells reduce the severity of acute lung injury in a sheep model of bacterial pneumonia. *Thorax* 2014; 69: 819-825.

8. Rojas M, Cardenes N, Kocyildirim E, Tedrow JR, Caceres E, Deans R, Ting A, Bermudez C. Human adult bone marrow-derived stem cells decrease severity of lipopolysaccharide-induced acute respiratory distress syndrome in sheep. *Stem Cell Res Ther* 2014; 5: 42.

AJRCCM Articles in Press. Published April 15, 2020 as 10.1164/rccm.201911-2143OC

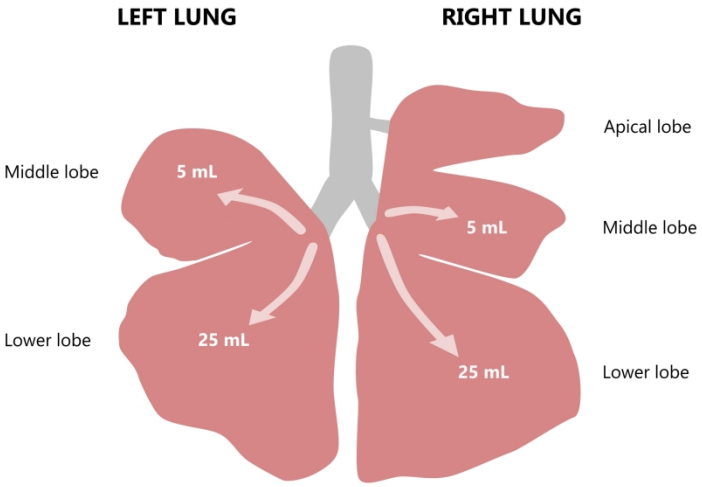

Figure E1

210x297mm (300 x 300 DPI)

AJRCCM Articles in Press. Published April 15, 2020 as 10.1164/rccm.201911-2143OC

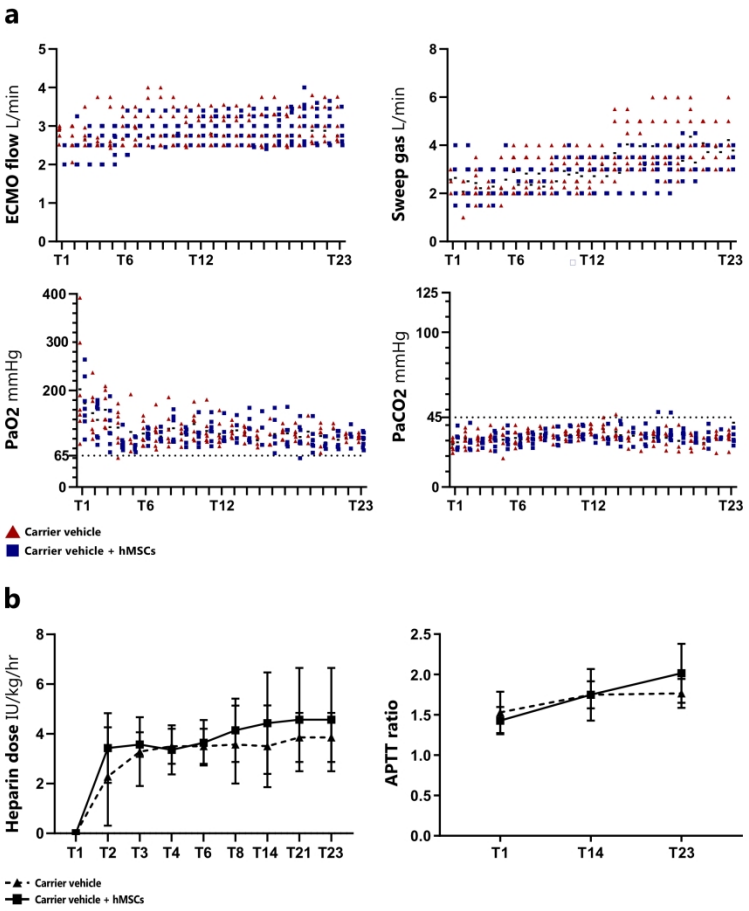

Figure E2

AJRCCM Articles in Press. Published April 15, 2020 as 10.1164/rccm.201911-2143OC

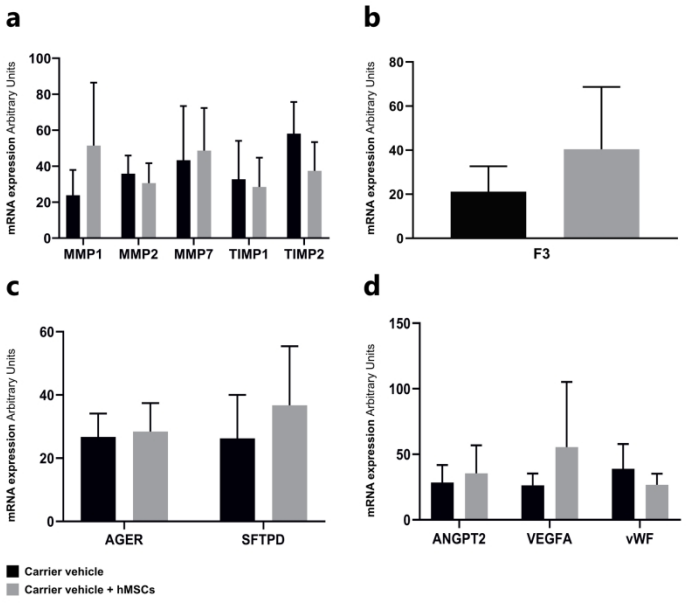

Figure E3

210x297mm (300 x 300 DPI)

AJRCCM Articles in Press. Published April 15, 2020 as 10.1164/rccm.201911-2143OC

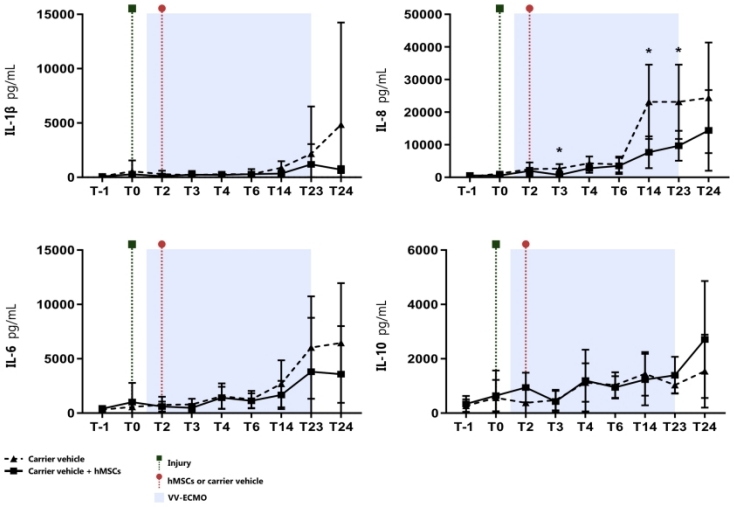

Figure E4

210x297mm (300 x 300 DPI)

AJRCCM Articles in Press. Published April 15, 2020 as 10.1164/rccm.201911-2143OC

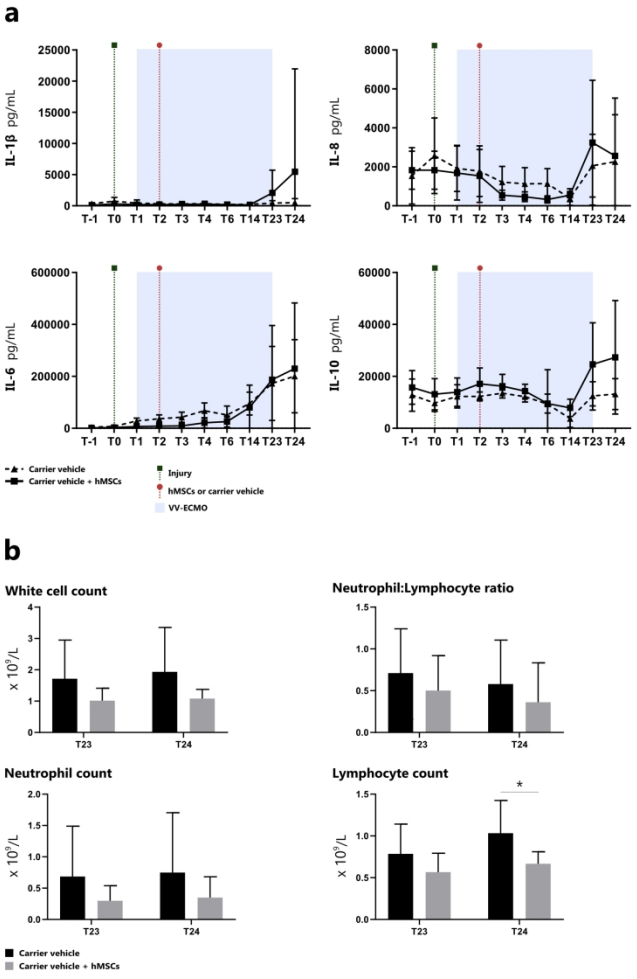

Figure E5

210x297mm (300 x 300 DPI)

AJRCCM Articles in Press. Published April 15, 2020 as 10.1164/rccm.201911-2143OC

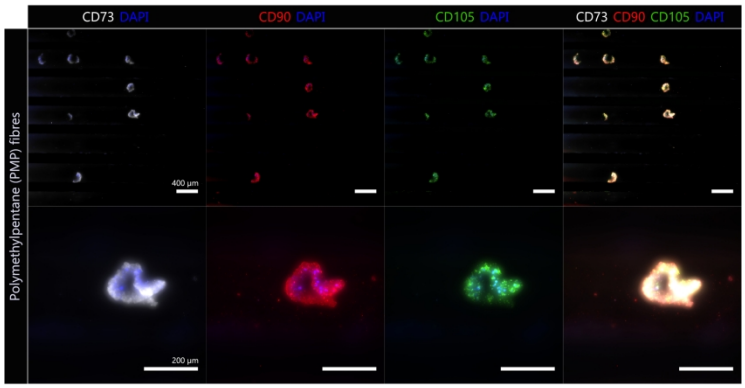

Figure E6

210x297mm (300 x 300 DPI)

AJRCCM Articles in Press. Published April 15, 2020 as 10.1164/rccm.201911-2143OC